



RESEARCH MEMORANDUM

AERODYNAMIC STUDY OF A WING-FUSELAGE COMBINATION
EMPLOYING A WING SWEPT BACK 63° - EFFECTIVENESS
OF AN INBOARD ELEVON AS A LONGITUDINAL- AND
LATERAL-CONTROL DEVICE AT SUBSONIC AND
SUPERSONIC SPEEDS

By Frank A. Pfyl

Ames Aeronautical Laboratory
Moffett Field, Calif.

NATIONAL ADVISORY COMMITTEE
FOR AERONAUTICS

WASHINGTON

December 4, 1951
Declassified April 8, 1957

NATIONAL ADVISORY COMMITTEE FOR AERONAUTICS

RESEARCH MEMORANDUM

AERODYNAMIC STUDY OF A WING-FUSELAGE COMBINATION
EMPLOYING A WING SWEPT BACK 63° - EFFECTIVENESS
OF AN INBOARD ELEVON AS A LONGITUDINAL- AND
LATERAL-CONTROL DEVICE AT SUBSONIC AND
SUPERSONIC SPEEDS

By Frank A. Pfyl

SUMMARY

The effectiveness of a 30-percent-chord, 50-percent semispan inboard elevon as a longitudinal- and lateral-control device for a wing-fuselage combination employing a wing swept back 63° has been determined experimentally. The investigation was made at Mach numbers of 0.6, 0.9, 1.2, 1.4, and 1.7 at a Reynolds number of 1.5 million. Data were also obtained at Reynolds numbers of 2.4 and 3.7 million to investigate dynamic-scale effects.

The results at supersonic speeds were compared with the experimental values obtained from tests conducted on a constant-percent-chord outboard elevon, and at subsonic speeds with data on a constant-chord outboard elevon. The lift effectiveness of the inboard elevon as indicated by $(CL_{\delta})_{\delta=0}$ was approximately twice that of the outboard elevon for the Mach number range investigated. This greater effectiveness of the inboard elevon may be attributed both to the greater separation effects over the outboard region of the wing promoted by the spanwise flow of the boundary layer on the swept-wing panel, and to the larger effect of induced lift on the wing panel due to the deflection of the inboard elevon. The pitching-moment effectiveness of the inboard elevon was, in general, greater at supersonic Mach numbers and less at subsonic speeds than that experienced by the outboard elevons; however, longitudinal control provided by either elevon was not adequate.

Sufficient lateral control was achieved by either elevon (rigid wing assumed) at the supersonic Mach numbers investigated; however, the superiority of the inboard elevon as a lateral-control device at supersonic speeds may be established by the fact that the effects of wing flexibility may reduce the rolling effectiveness of the outboard elevon as much as 50 percent from those for a rigid wing.

INTRODUCTION

For the past few years, considerable emphasis has been placed on the optimum spanwise location of flap-type control surfaces on swept-back wings. Tests at both subsonic and supersonic speeds (references 1, 2, 3, and 4) have shown that an outboard elevon on a 63° swept-back wing does not develop its potential effectiveness. Subsequent studies have indicated that the longitudinal-and lateral-control characteristics of an elevon on highly swept wings could be improved by placing the elevon in an inboard position where the effects of flow separation and elastic deformation of the wing would be less severe than for an outboard position. Accordingly, the characteristics of a wing similar to the wings of references 1, 2, and 3, but having an inboard elevon, have been investigated at Mach numbers of 0.6, 0.9, 1.2, 1.4, and 1.7 to provide additional information on the optimum location of control flaps on highly swept wings. The results of this investigation are presented herein and are compared with the results of references 1, 2, and 3.

NOTATION

The following symbols were used in this report:

C_L	lift coefficient	$\left(\frac{\text{lift}}{qS} \right)$
C_D	drag coefficient	$\left(\frac{\text{drag}}{qS} \right)$
C_m	pitching-moment coefficient about quarter-chord point of wing	
	mean aerodynamic chord	$\left(\frac{\text{pitching moment}}{qS\bar{c}} \right)$
C_l	rolling-moment coefficient	$\left(\frac{\text{rolling moment}}{qSb} \right)$
C_h	hinge-moment coefficient	$\left(\frac{\text{hinge moment}}{2qM_A} \right)$
$C_{L\delta}$	elevon lift-effectiveness parameter for constant angle of attack measured at $\delta = 0$	$\left(\frac{\partial C_L}{\partial \delta} \right)_a$, per degree
$C_{m\delta}$	elevon pitching-moment-effectiveness parameter for constant angle of attack measured at $\delta = 0$	$\left(\frac{\partial C_m}{\partial \delta} \right)_a$, per degree

$C_{h\alpha}$ rate of change of hinge-moment coefficient with change in angle of attack for constant angles of elevon deflection measured at

$$\alpha = 0 \left(\frac{\partial C_h}{\partial \alpha} \right)_{\delta}, \text{ per degree}$$

$C_{h\delta}$ rate of change of hinge-moment coefficient with change in elevon deflection for constant angle of attack measured at

$$\delta = 0 \left(\frac{\partial C_h}{\partial \delta} \right)_{\alpha}, \text{ per degree}$$

$C_{l\delta}$ elevon rolling-moment-effectiveness parameter for constant angle of attack measured at $\delta = 0 \left(\frac{\partial C_l}{\partial \delta} \right)_{\alpha}$, per degree

C_l damping-moment coefficient in roll, rate of change of rolling-moment C_l with wing-tip helix angle $\frac{pb}{2V}$, per radian

M Mach number

M_A first moment of area of elevon surface aft of hinge line, feet cubed

R Reynolds number, based on mean aerodynamic chord

S wing area, including area within body, square feet

V free-stream velocity, feet per second

b wing span, feet

c local wing chord measured parallel to plane of symmetry, feet

\bar{c} wing mean aerodynamic chord $\left(\frac{\int_0^{b/2} c^2 dy}{\int_0^{b/2} c dy} \right)$, feet

p angular velocity in roll, radians per second

$\frac{pb}{2V}$ wing-tip helix angle, radians

q free-stream dynamic pressure, pounds per square foot

x, y rectangular coordinates

α angle of attack of fuselage center line, degrees

δ angle between wing chord and elevon chord measured in a plane perpendicular to the elevon hinge line, positive for downward deflection with respect to the wing, degrees

δ_{nom} nominal elevon deflection angle determined by position of the hexagonal strain-gage torque arm, degrees

APPARATUS

Tunnel

The experimental investigation was conducted in the Ames 6- by 6-foot supersonic wind tunnel. In this wind tunnel, the Mach number may be varied continuously from 0.6 to 0.95 and from 1.2 to 1.7 and the stagnation pressure can be regulated to maintain a constant test Reynolds number. Further information on this wind tunnel is presented in reference 5.

Balance

A four-component, electrical, strain-gage balance supported by a sting and enclosed within the fuselage of the model was used to measure the aerodynamic forces and moments of the model. The strain-gage balances and instrumentation are described in detail in reference 1.

Model

The model used in the present investigation consisted of a wing-fuselage combination employing a wing of aspect ratio 3.5, taper ratio 0.25, and having 63° sweepback of the leading edge. Sections perpendicular to the leading edge were the NACA 0010. The wing was mounted centrally with 0° incidence on the fuselage. A sketch of the model showing plan-form dimensions is presented in figure 1. The wing-fuselage configuration was identical to the plane wing-fuselage configuration used in references 1 and 2, except for the location of the elevon. For the present investigation, the elevon was located on the left wing panel and extended from the wing-body juncture to the 50-percent semispan station. The elevon was aerodynamically unbalanced and was hinged along the 70-percent wing-chord station measured parallel to the plane of symmetry. The areas of this elevon and the areas of the elevons of references 1, 2, and 3 are presented in table 1.

An electrical strain-gage hinge-moment balance was mounted in the left wing panel at the 50-percent semispan station. (See fig. 1.)

The model was sting mounted in the tunnel. (See fig. 2.)

TESTS AND PROCEDURE

Range of Test Variables

Measurements of the lift, drag, pitching moment, rolling moment, and hinge moment were made for Mach numbers of 0.6, 0.9, 1.2, 1.4, and 1.7 at a Reynolds number of 1.5 million. An investigation of possible dynamic scale effect was made which included data at Reynolds numbers of 2.4 and 3.7 million at the above-mentioned Mach numbers. The angle of attack was varied from -4° to the maximum positive angle attainable in increments of 2° and experimental data were obtained for elevon deflections of 0° , $\pm 10^\circ$, $\pm 20^\circ$, and $\pm 25^\circ$.

Corrections to and Reduction of the Data

In the supersonic Mach number range, the test data were reduced and the corrections applied in the same manner as for references 1 and 2. For subsonic speeds, the effects of tunnel-wall interference, stream variation, and support interference have been fully discussed in reference 6. The corrections discussed in reference 6 were applied to the present data with appropriate modifications of the constants in the expressions for tunnel-wall interference. The values used in this test were:

$$\Delta\alpha = 0.581 C_L$$

$$\Delta C_D = 0.0101 C_L^2$$

Precision of the Data

The uncertainties involved in determining dynamic pressure and in measuring forces with the strain-gage balance have been previously discussed in references 1, 2, and 7. The uncertainties of the measured aerodynamic parameters are given as follows:

<u>Quantity</u>	<u>Uncertainty</u>
Lift coefficient	0.003
Drag coefficient	0.001
Pitching-moment coefficient	0.001
Rolling-moment coefficient	0.0008
Hinge-moment coefficient	0.002
Mach number	0.01
Reynolds number	0.03×10^6
Angle of attack	0.1°
Elevon-deflection angle	0.25°

RESULTS AND DISCUSSION

Reynolds Number Effect

The effect of Reynolds number on the aerodynamic characteristics of the wing-fuselage combination is presented in figure 3. These data were presented for 0° and 25° nominal elevon deflection at 0.9 and 1.7 Mach numbers and Reynolds numbers of 1.5, 2.4, and 3.7 million.¹ This preliminary investigation showed no marked scale effect on the basic parameters in this Reynolds number range. Therefore, the remainder of the test was conducted at a Reynolds number of 1.5 million.

Control-Surface Effectiveness

The aerodynamic characteristics at Mach numbers of 0.6, 0.9, 1.2, and 1.7 are presented in figure 4. (The data for 1.4 Mach number were omitted, except in the final figures, since the data at 1.2 and 1.7 Mach numbers show representative results.) Only representative test conditions were given in figure 4 since elevon-deflection angles varied due to aerodynamic loading (as much as $\pm 1.0^\circ$); consequently, the data shown in figure 4 are for nominal elevon deflections of 0° and $\pm 25^\circ$ only. To present the data in a more usable form, C_L , C_D , C_m , C_l , and C_h were cross-plotted as a function of elevon-deflection angle (corrected for deflections under load) for constant angle of attack up to approximately 14° and are given in figures 5, 6, 7, 8, and 9. The data in these figures are presented in 2° increments of angle of attack where clarity of the figures permits.

¹Data were also obtained at 0.6, 1.2, and 1.4 Mach numbers, but were not presented since the data presented show representative results.

The discussion will be mainly devoted to the effectiveness parameters CL_δ , CM_δ , Ch_α , Ch_δ , and $C_{l\delta}$ (measured at $\delta = 0^\circ$) shown in figures 10, 11, 12 and 13, respectively, and to figures 14 and 15 which are concerned with the rolling effectiveness of the control as measured by the attainable wing-tip helix angle, $pb/2V$. These figures present data for deflection of two elevons.

Comparisons of the data of the present investigation are made with the data of references 1 and 2 for supersonic speeds in figures 10, 11, 13, 14, and 15, and with reference 3 for subsonic speeds in figures 10 and 11. The data obtained from references 1 and 2 are for the same wing-body configuration, but with a 30-percent-chord, 50-percent semispan outboard elevon, and the data taken from reference 3 were for a comparable wing-body configuration² with a constant-chord 50-percent semispan outboard elevon.

Lift.- The variation of the lift-effectiveness parameter, CL_δ , with Mach number is presented in figure 10. In the subsonic speed range, the data for the inboard elevon show somewhat higher values of CL_δ throughout the angle-of-attack range at a Mach number of 0.9 than at a Mach number of 0.6. It may also be noted that the lift effectiveness increased with increasing angles of attack at each subsonic Mach number investigated. A comparison is shown in figure 10 of the results of reference 3 (constant-chord 50-percent semispan outboard elevon) with the data for the inboard elevon for 0° angle of attack at subsonic Mach numbers. The inboard elevon has approximately twice the lift effectiveness of the outboard elevon of reference 3. This difference in CL_δ may be attributed both to the greater separation effects over the outboard region of the wing promoted by the spanwise flow of the boundary layer on the swept-wing panel, and to the larger effect of induced lift on the wing panel due to the deflection of the inboard elevon.³

The inboard elevon showed a noticeable loss in lift effectiveness between a Mach number of 0.9 and 1.2. The outboard elevon showed only a small loss in lift effectiveness between the Mach numbers of 0.9 and 1.2.

²For the wing of reference 3, the airfoil sections in a streamwise plane were the NACA 64A006.

³The wing used in this investigation and in references 1 and 2 was very rigid, thus permitting no aeroelastic effects; however, the wing used in reference 3 was not so rigid - no attempt being made to measure the wing elasticity; consequently, the influence of aeroelasticity could account for some loss in lift effectiveness.

For the supersonic Mach numbers investigated, the data presented in figure 10 show a higher lift effectiveness for the inboard elevon than that for the constant-percent-chord outboard elevon of reference 1. The greater lift effectiveness of the inboard elevon may, as in the subsonic case, be attributed both to the relative decrease in separation effects along the inboard region of the wing, and to the larger effect of induced lift on the wing panel due to the deflection of the inboard elevon. Tuft pictures of the entire wing presented in reference 1 show complete flow separation (see reference 8 for discussion of separation) over the region occupied by the outboard elevon at all supersonic Mach numbers for angles of attack of 6° and greater; whereas the separation effects are shown to be much less severe over the region of the wing where the inboard elevon was located. These separation effects would seem to account for the greater effectiveness of the inboard control surface and the rapid decrease in lift effectiveness for the outboard elevon with increasing angles of attack at supersonic speeds. Figure 10 also shows that the lift effectiveness for both elevons decreased with increasing supersonic Mach number; however, the lift effectiveness of the inboard elevon decreased more rapidly with increasing Mach number than that of the outboard control surface.

Pitching moment.- The pitching-moment curves presented in figure 4 exhibit a decrease in stability at the higher angles of attack which is primarily dependent upon the sweep angle and aspect ratio of the wing. (See reference 9.) A forward shift of the center of pressure of the load on the wing as the angle of attack was increased occurred at a lift coefficient of the order of 0.35, depending upon the elevon-deflection angle and Mach number.

Figure 11 shows the variation of pitching-moment-effectiveness parameter, $C_{m\delta}$, with Mach number. For subsonic speeds, the pitching-moment effectiveness for the inboard elevon at a Mach number of 0.9 is greater than that at a Mach number of 0.6 for angles of attack up to 10° . The effect of increasing the angle of attack from 0° to 6° at a Mach number of 0.6 was to increase the pitching-moment effectiveness; whereas, at a Mach number of 0.9, $C_{m\delta}$ decreased with increasing angle of attack. A comparison of the data at 0° angle of attack with the data of reference 3 (constant-chord outboard elevon) shows less pitching-moment effectiveness for the inboard elevon, a result that would be expected since the moment arm for the outboard elevon of reference 3 would be approximately four times that of the inboard elevon.

An increase in pitching-moment effectiveness was noted between a Mach number of 0.9 and 1.2 for the inboard elevon. Since $C_{L\delta}$ decreased between these Mach numbers, a rearward shift in the center of pressure of the load due to elevon deflection is indicated.

For the supersonic speeds, the data shown in figure 11 for the inboard elevon indicate, generally, larger values of $C_{m\delta}$ than that of

the outboard elevon. From the data in figure 11, it can be seen that both elevons exhibit losses in $C_{m\delta}$ with increasing supersonic Mach number at 1° and 6° angles of attack, whereas the reverse was true at 10° angle of attack. The ability of either elevon to produce an incremental pitching-moment coefficient decreased with increasing angle of attack at 1.2 Mach number. This trend was sustained throughout the supersonic Mach number range for the outboard elevon; however, the data for the inboard elevon at a Mach number of 1.4 show an increase in $C_{m\delta}$ with increasing angle of attack up to 6° . At 1.7 Mach number, the data show an increase in $C_{m\delta}$ up to 10° angle of attack.

An evaluation of the capabilities of the outboard elevon as a sole means of trimming a tailless airplane of the present configuration was made in reference 1. It was found that the longitudinal control provided was inadequate for supersonic flight of this wing-fuselage combination. Since the inboard elevon indicated insufficient increases in $C_{m\delta}$ over that of the outboard elevon, additional means of providing longitudinal control would still be necessary for supersonic flight of this wing-fuselage combination.

Elevon hinge moment.- Figure 12 presents the variation with Mach number of the rate of change of hinge-moment coefficient with change in elevon deflection, $C_{h\delta}$, for constant angles of attack, and with change in angle of attack, $C_{h\alpha}$, for constant angles of elevon deflection. The data show that, in general, the effect of increasing the Mach number was to increase the tendency for the elevon to return to the undeflected position.

Rolling moment.- The variation of the rolling-moment-effectiveness parameter, $C_{l\delta}$, with Mach number is presented in figure 13. The effect of increasing the Mach number from 0.6 to 0.9 was to increase the rolling-moment effectiveness. An increase in $C_{l\delta}$ with increasing angle of attack occurred at the subsonic Mach numbers investigated.

For the inboard elevon, $C_{l\delta}$ increased between 0.9 and 1.2 Mach numbers, with the exception of the data presented for 10° angle of attack. Since a noticeable loss in $C_{l\delta}$ and a gain in $C_{m\delta}$ were also observed through this speed range, an outboard and rearward movement in the center of pressure of the load occurred.

For the supersonic speed range, it is evident from the data presented in figure 13 that the inboard elevon is more effective in roll than the outboard elevon. The variation of $C_{l\delta}$ with Mach number for

the inboard control surface was similar to that of the outboard elevon; however, an increase in $C_{l\delta}$ for the inboard elevon occurred with increasing angle of attack up to 5° ; whereas for the outboard elevon, $C_{l\delta}$ decreased with angle of attack.

A good quantitative indication of the adequacy (reference 10) of an elevon as a lateral-control device can be obtained from computed values of the rolling-effectiveness parameter $\frac{pb}{2V}$. The variation of $\frac{pb}{2V}$ with Mach number is presented in figure 14 for 0° angle of attack.

The values of $\frac{pb}{2V}$ shown in figure 14 were calculated, utilizing the same values of damping-moment coefficient in roll, C_{l_p} , for supersonic speeds as used in reference 2. At subsonic speeds, C_{l_p} was computed by the method of reference 11. Table 2 presents the values of C_{l_p} used. (Reference 12 was used to obtain the values of average section lift coefficient required in applying the methods of reference 11.)

For airplanes capable of very high speeds, the maximum rolling velocity is believed to be more of a criterion of the required rolling performance⁴ than $pb/2V$. A comparison of the $pb/2V$ obtained from 40° total elevon deflection at 0° angle of attack with that required to attain a rolling velocity of 220° per second with a 40-foot-wing-span airplane flying at 60,000 feet is made in figure 15. The results show that either elevon in the supersonic speed range could be reduced in size if used as ailerons only (rigid wing assumed). Calculations of reference 2 indicated that, because of wing flexibility, as much as a 50-percent reduction in the outboard aileron effectiveness in roll from rigid-wing values could occur because of structural deformation. Consequently, the inboard elevon with its tendency for less structural deflection of the wing when deflected appears to be a better lateral-control device than the outboard elevon for this wing-fuselage configuration. (See also reference 4.) It should be noted also that the inboard elevon provided adequate lateral control within the range of subsonic speeds investigated.

⁴For the type of airplane under consideration, Army and Navy specifications require a $pb/2V = 0.09$, or that the peak rolling rate need never exceed 220° per second. (See reference 10.)

CONCLUSIONS

The results of the investigation of the effectiveness of a constant-percent-chord inboard elevon as a longitudinal- and lateral-control device for the 63° swept-wing body configuration, when compared with results for an outboard aileron, revealed the following:

1. The lift effectiveness of the inboard elevon as indicated by $(C_{L\delta})_{\delta=0}$ was approximately twice that of the outboard elevon for the Mach number range investigated. This greater effectiveness of the inboard elevon may be attributed both to the greater separation effects over the outboard region of the wing promoted by the spanwise flow of the boundary layer of the swept-wing panel, and to the larger effect of induced lift on the wing panel due to the deflection of the inboard elevon.
2. The pitching-moment effectiveness of the inboard elevon was, in general, greater at supersonic Mach numbers and less at subsonic speeds than that of the outboard elevon; however, longitudinal control provided by either elevon was not adequate.
3. Sufficient lateral control was achieved by either elevon for the supersonic Mach numbers investigated (rigid wing assumed). However, the superiority of the inboard elevon as a lateral-control device at supersonic speeds may be established by the fact that aeroelastic effects due to wing flexibility may reduce the rolling effectiveness of the outboard elevon as much as 50 percent from that of a rigid wing.

Ames Aeronautical Laboratory,
National Advisory Committee for Aeronautics,
Moffett Field, Calif.

REFERENCES

1. Olson, Robert N., and Mead, Merrill H.: Aerodynamic Study of a Wing-Fuselage Combination Employing a Wing Swept Back 63° - Effectiveness of an Elevon as a Longitudinal Control and the Effects of Camber and Twist on the Maximum Lift-Drag Ratio at Supersonic Speeds. NACA RM A50A31a, 1950.

2. Olson, Robert N., and Mead, Merrill H.: Aerodynamic Study of a Wing-Fuselage Combination Employing a Wing Swept Back 63° - Effectiveness at Supersonic Speeds of a 30-Percent Chord, 50-Percent Semispan Elevon as a Lateral Control Device. NACA RM A50K07, 1951.
3. Reynolds, Robert M., and Smith, Donald W.: Aerodynamic Study of a Wing-Fuselage Combination Employing a Wing Swept Back 63° .- Subsonic Mach and Reynolds Number Effects on the Characteristics of the Wing and on the Effectiveness of an Elevon. NACA RM A8D20, 1948.
4. Strass, H. Kurt, Fields, E. M., and Schult, Eugene D.: Some Effects of Spanwise Aileron Location and Wing Structural Rigidity on the Rolling Effectiveness of 0.3-Chord Flap-Type Ailerons on a Tapered Wing having 63° Sweepback at the Leading Edge and NACA 64A005 Airfoil Sections. NACA RM L51D18a, 1951.
5. Frick, Charles W., and Olson, Robert N.: Flow Studies in the Asymmetric Adjustable Nozzle of the Ames 6- by 6-foot Supersonic Wind Tunnel. NACA RM A9E24, 1949.
6. Reese, David E., Jr., and Phelps, E. Ray: Lift, Drag, and Pitching Moment of Low-Aspect-Ratio Wings at Subsonic and Supersonic Speeds - Plane Tapered Wing of Aspect Ratio 3.1 with 3-Percent-Thick, Biconvex Section. NACA RM A50K28, 1951.
7. Hall, Charles F., and Heitmeyer, John C.: Aerodynamic Study of a Wing-Fuselage Combination Employing a Wing Swept Back 63° - Characteristics at Supersonic Speeds of a Model With the Wing Twisted and Cambered for Uniform Load. NACA RM A9J24, 1949.
8. Jones, Robert T.: Effects of Sweepback on Boundary Layer and Separation. NACA Rep. 884, 1947. (Formerly NACA TN 1402)
9. Shortal, Joseph A., and Maggin, Bernard: Effect of Sweepback and Aspect Ratio on Longitudinal Stability Characteristics of Wings at Low Speeds. NACA TN 1093, 1946.
10. U.S. Air Force Specification No. 1815-B: Flying Qualities of Piloted Airplanes. June 1, 1948.
11. DeYoung, John: Theoretical Antisymmetric Span Loading for Wings of Arbitrary Plan Form at Subsonic Speeds. NACA TN 2140, 1950.
12. Polentz, Perry P.: Comparison of the Aerodynamic Characteristics of the NACA 0010 and 0010-64 Airfoil Sections at High Subsonic Mach Numbers. NACA RM A9G19, 1950.

TABLE 1.- ELEVON AREAS

Reference	Area, one elevon (ft sq)	Flap area
		Total wing area (percent)
This report	0.148	12.2
1 and 2	.124	10.2
3	1.786	12.5

TABLE 2.- VALUES OF C_{l_p} USED IN
COMPUTING VALUES OF $P_b/2V$

Mach number	Angle of attack (deg)	C_{l_p}
0.6	0	-0.1935
.9	0	-.1986
1.2	0	-.2521
1.4	0	-.2690
1.7	0	-.2817



Page intentionally left blank

Page intentionally left blank

Aspect ratio 3.50 Airfoil section perpendicular to leading edge: NACA 0010

Taper ratio 0.25

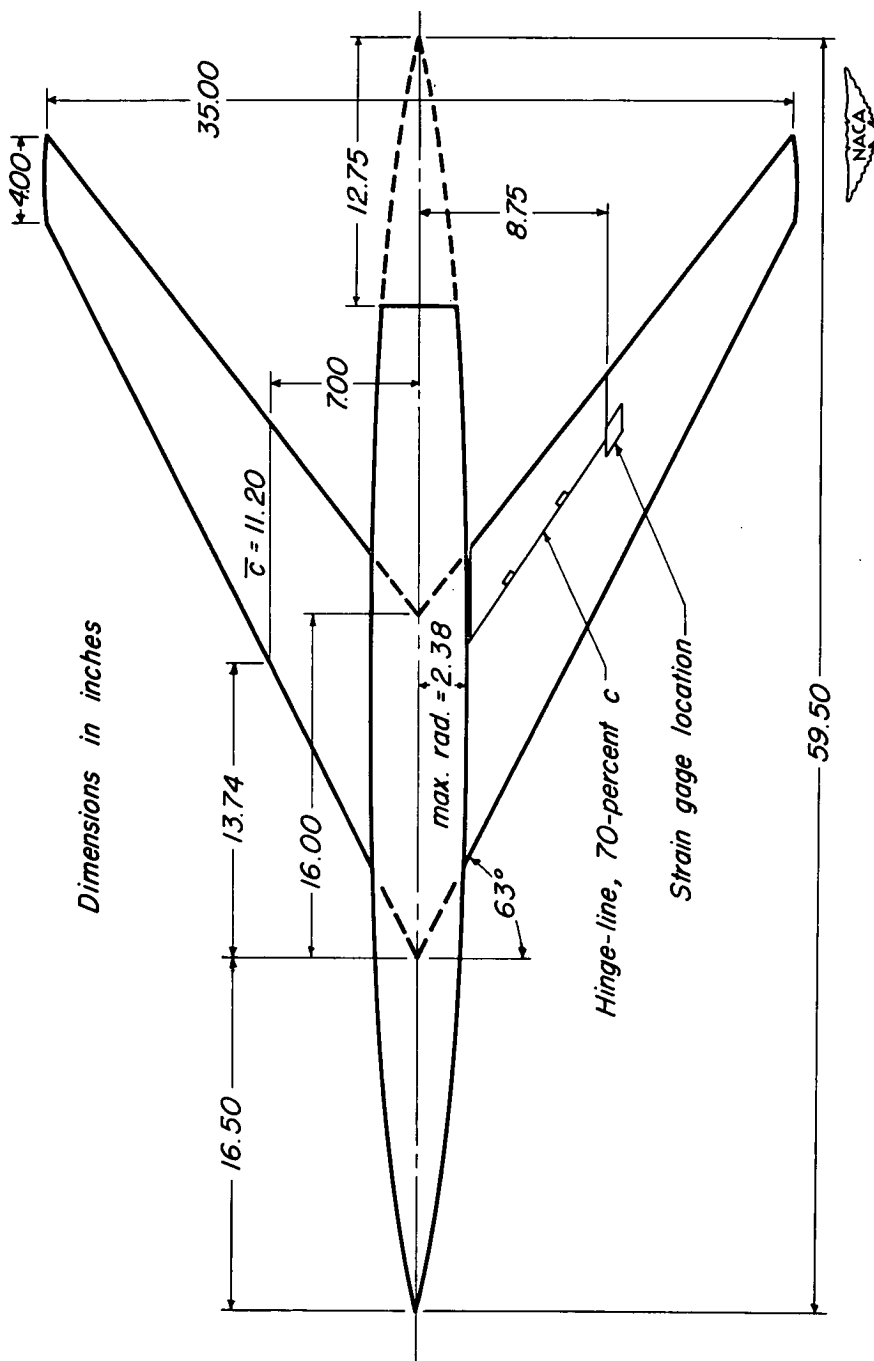


Figure 1. - Sketch of model showing principal dimensions and location of elevon.



Figure 2.- The model showing positive elevon deflection in the Ames 6- by 6-foot supersonic wind tunnel.

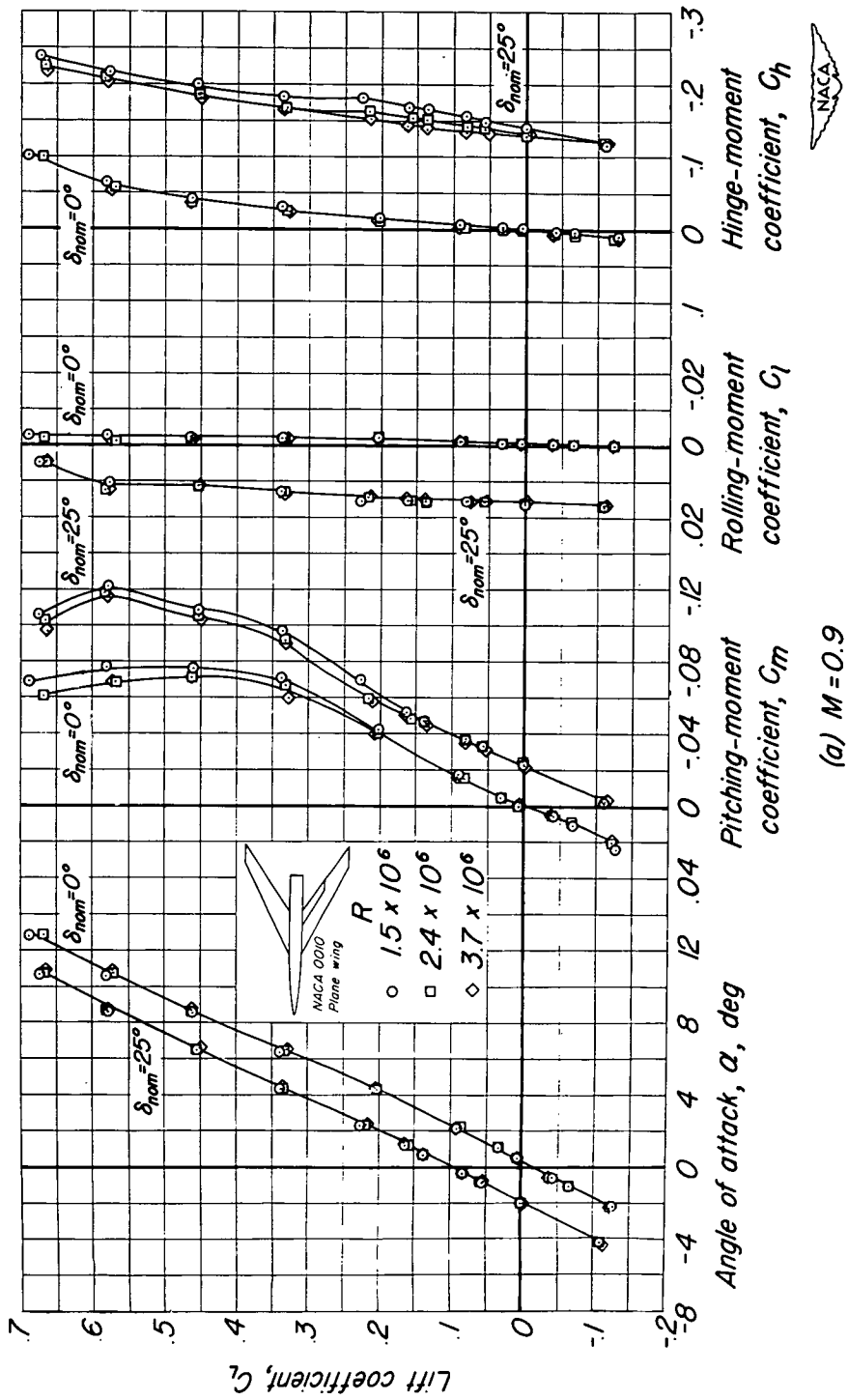


Figure 3.- Effect of Reynolds number on the aerodynamic characteristics of a 63° swept-back wing-fuselage combination at two Mach numbers for 0° and 25° elevon deflections. Data for one elevon.

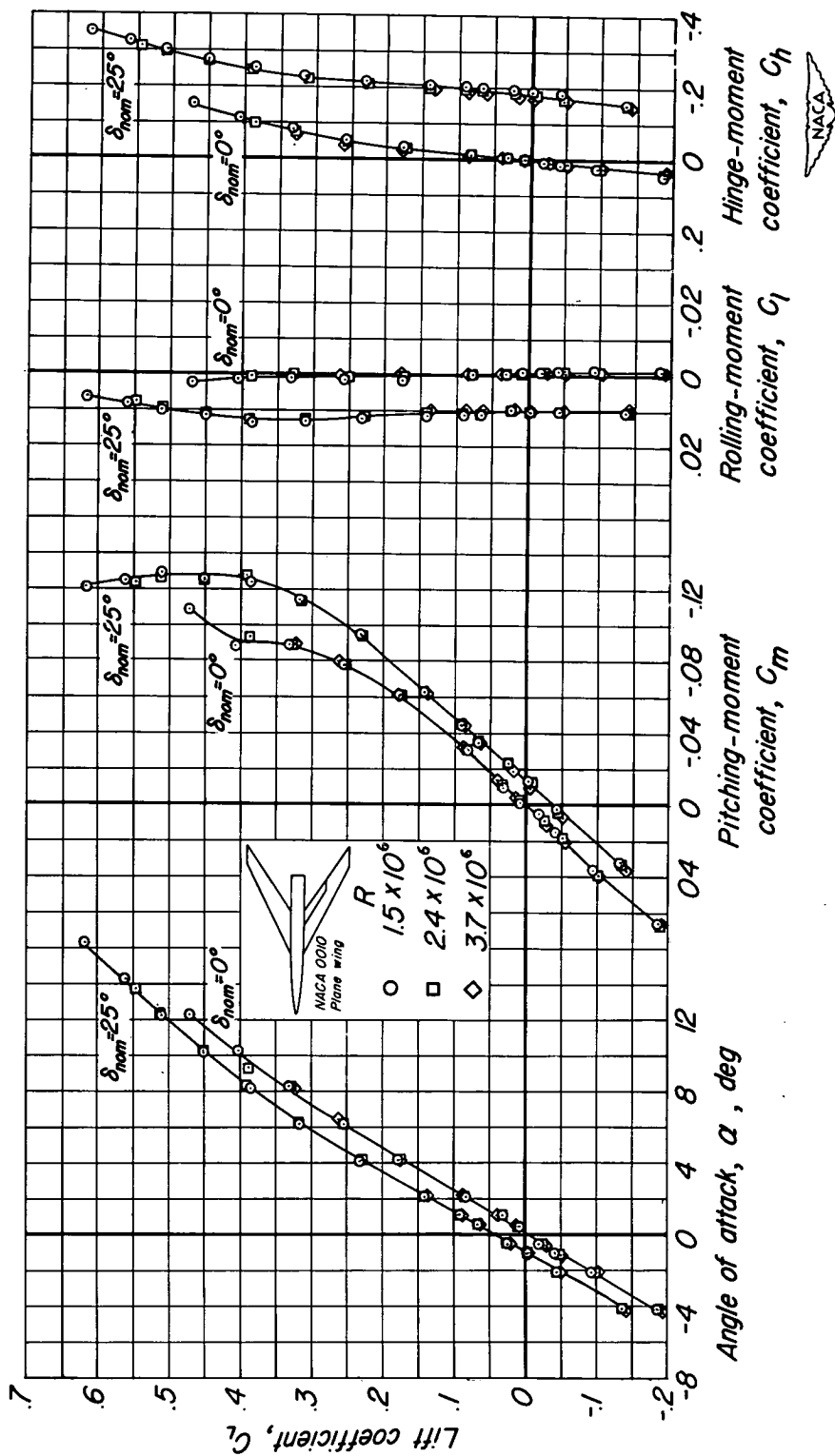


Figure 3.-Concluded.

(b) $M = 1.7$

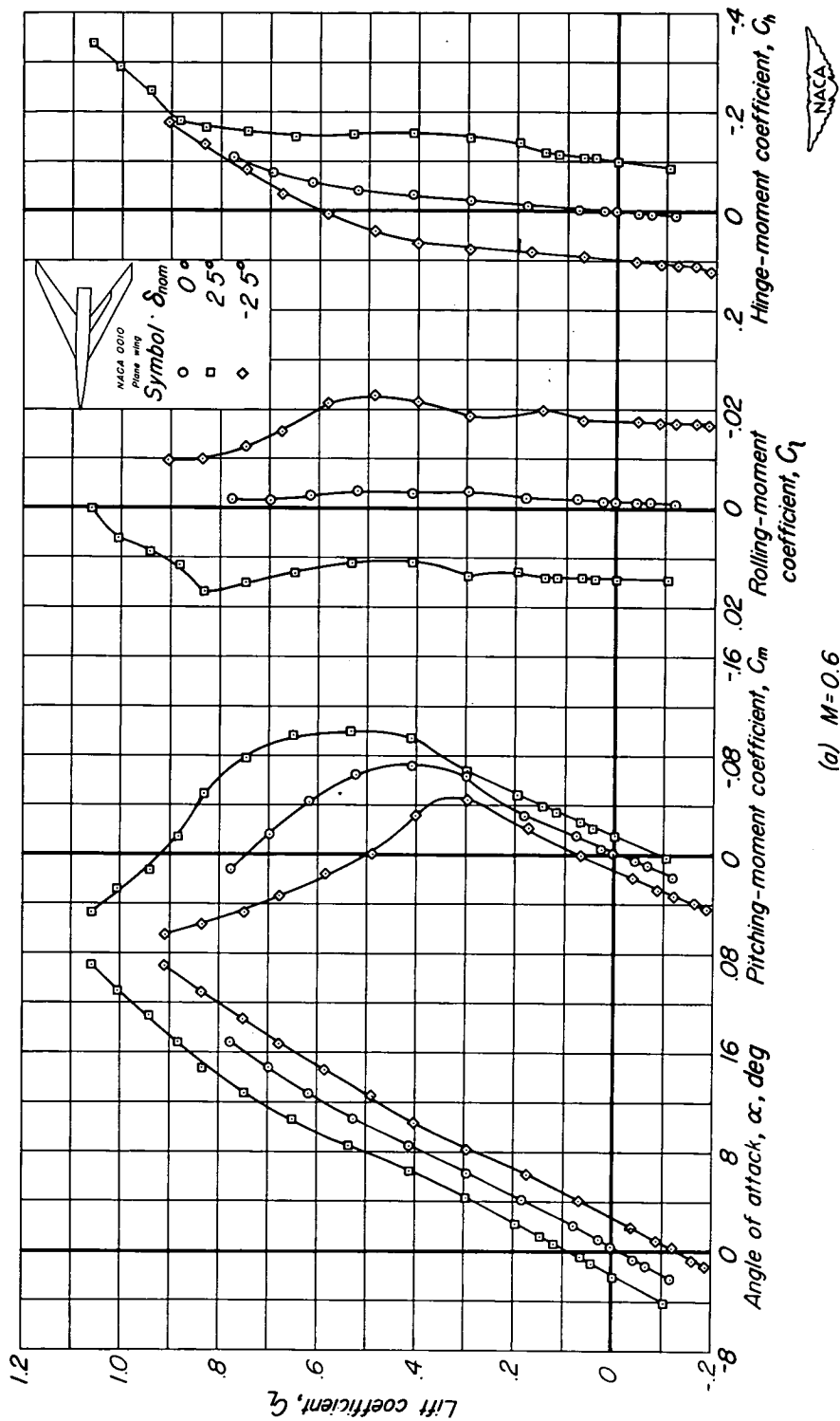


Figure 4 - Effect of elevon deflection on the aerodynamic characteristics of a 6.3° swept-back wing-fuselage combination at various Mach numbers. Data for one elevon. $R = 1.5 \times 10^6$.

Mach numbers. Data for one elevon. $R = 1.5 \times 10^6$.

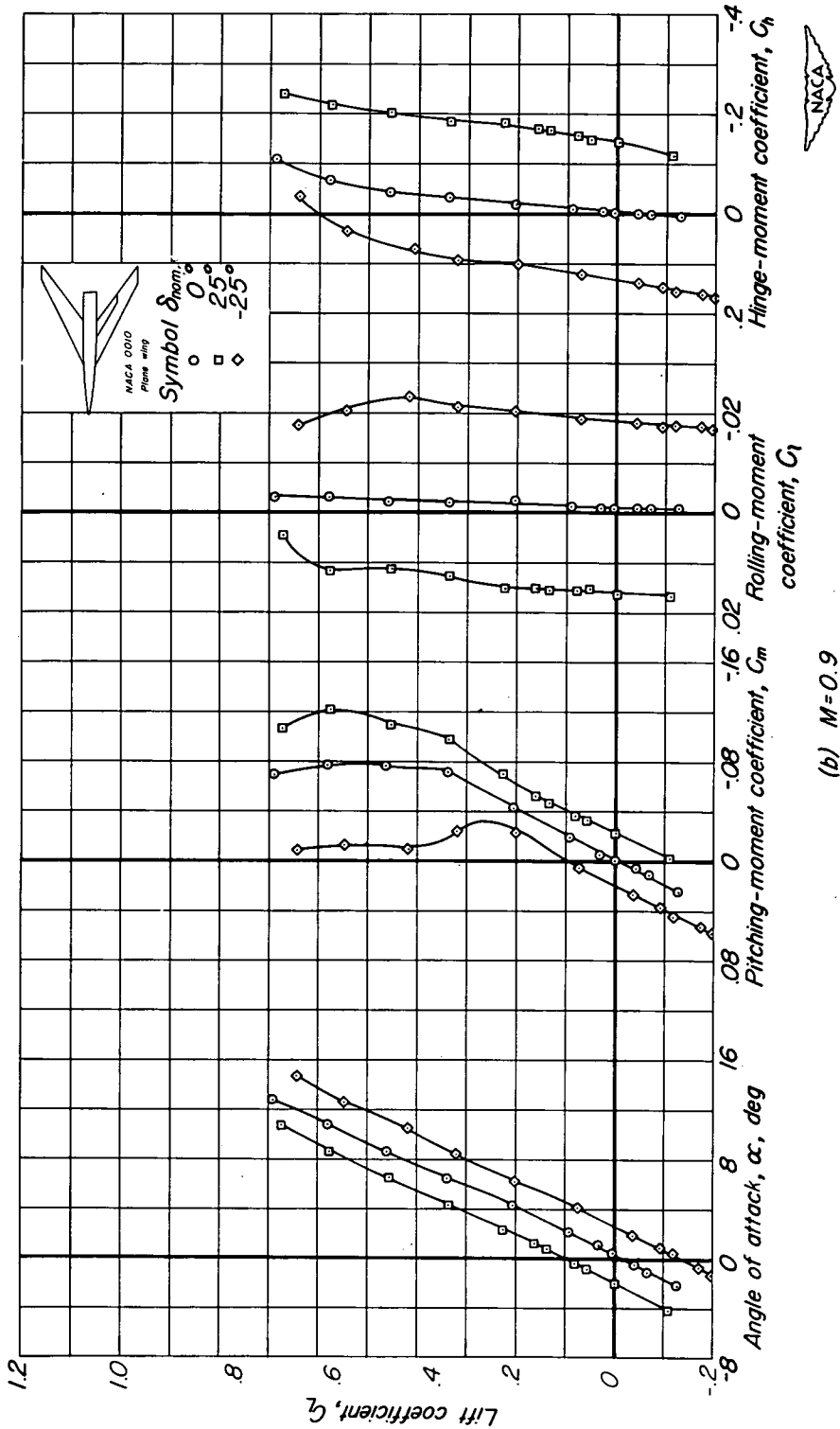


Figure 4. -Continued.

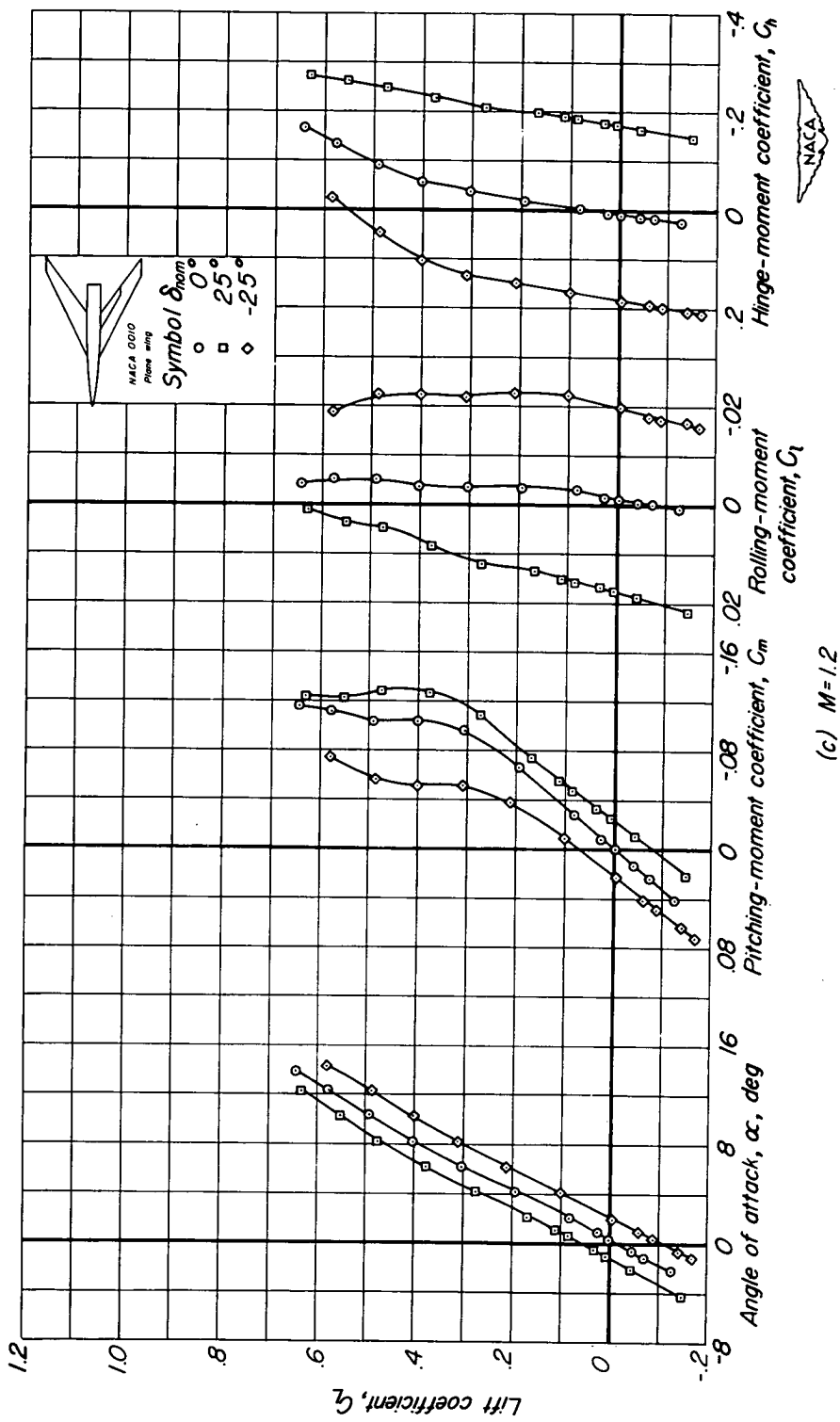


Figure 4 - Continued.

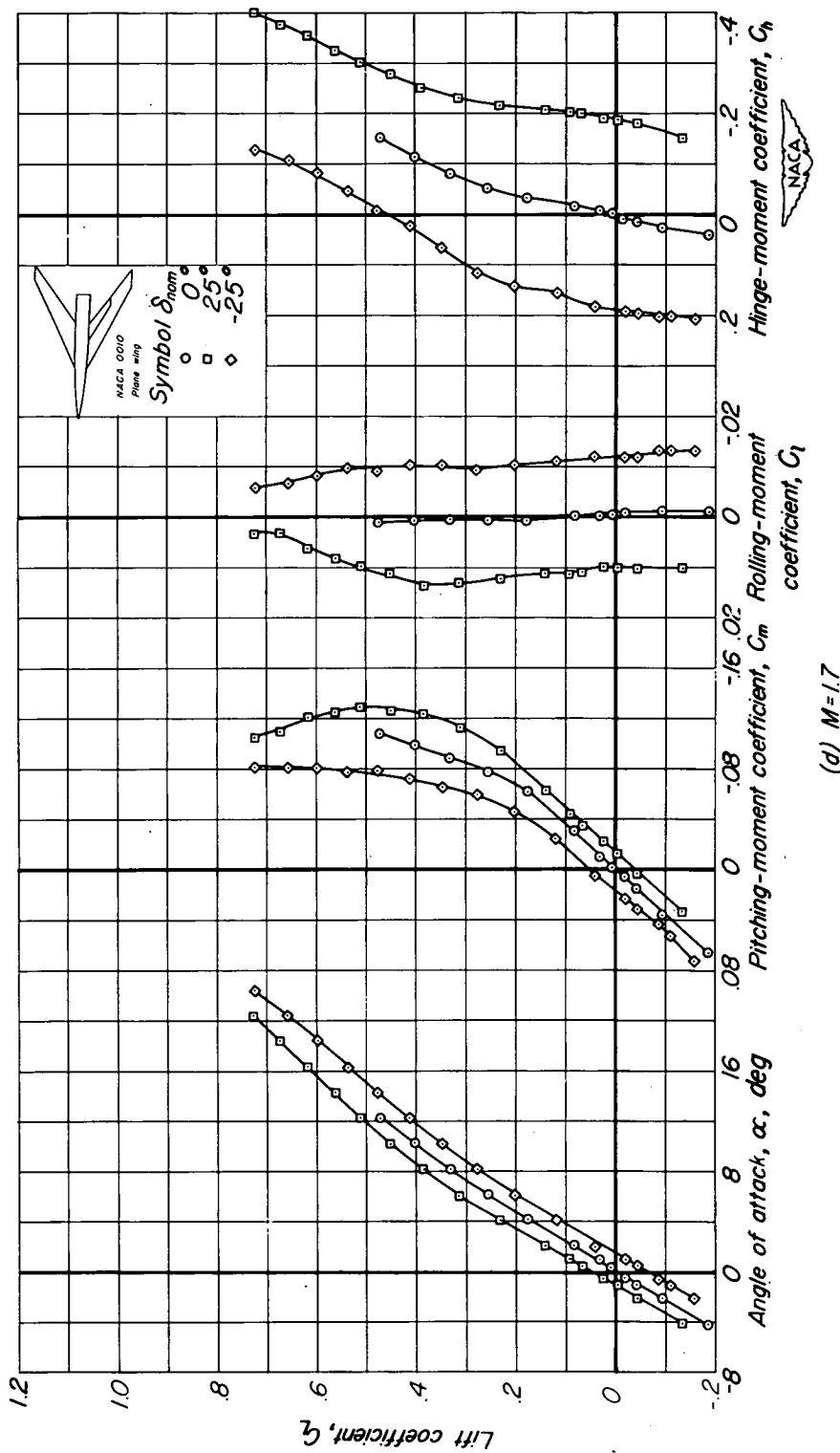


Figure 4. -Concluded.

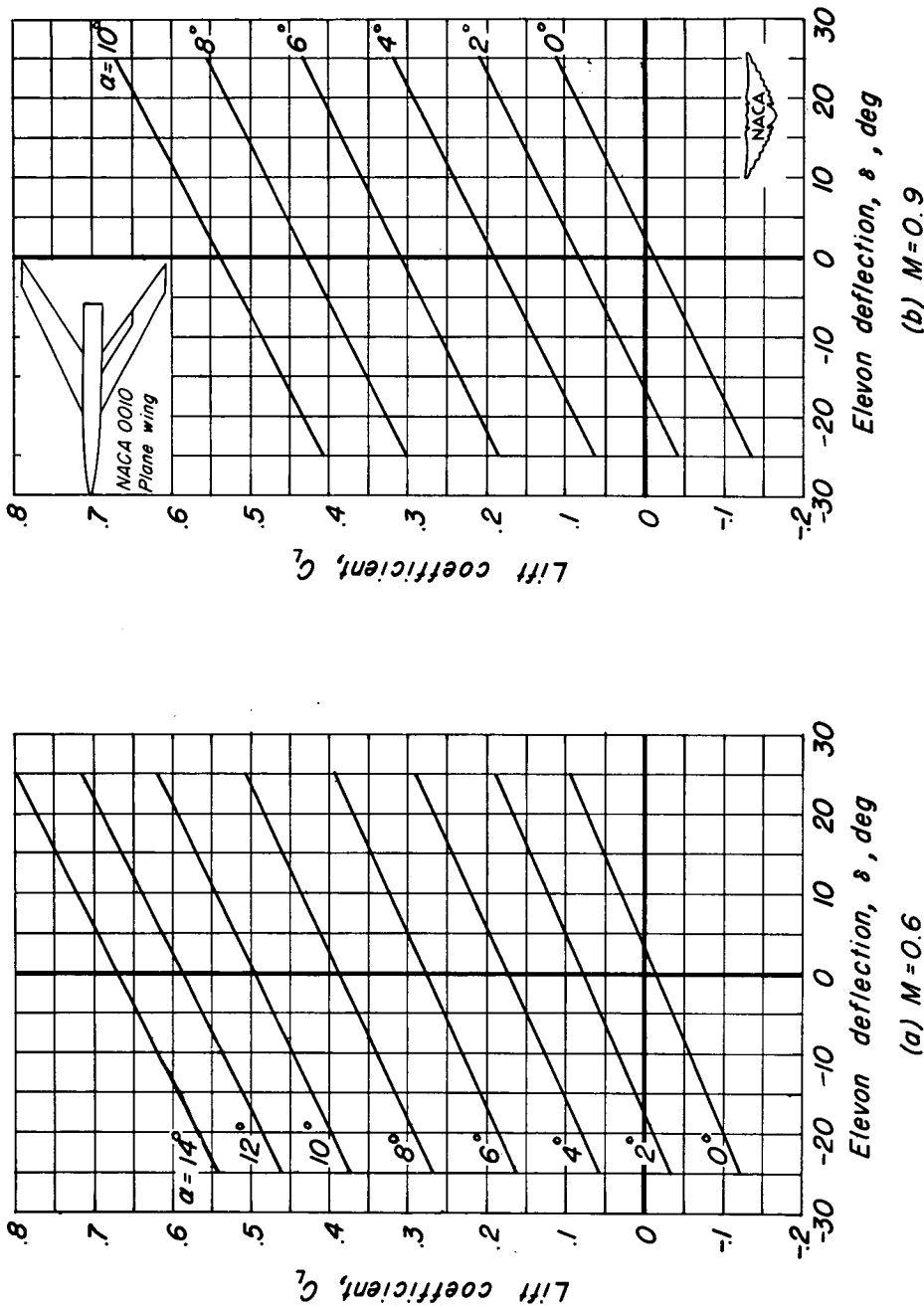


Figure 5 - Variation of lift coefficient with elevon deflection at various Mach numbers. Data for one elevon. $R = 1.5 \times 10^6$.

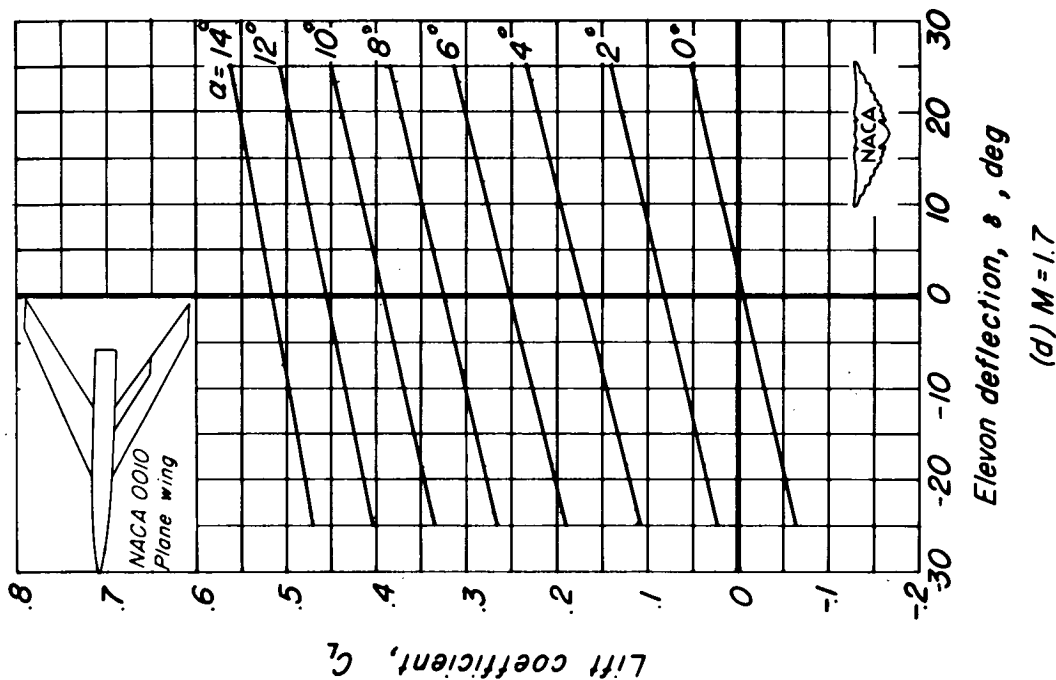
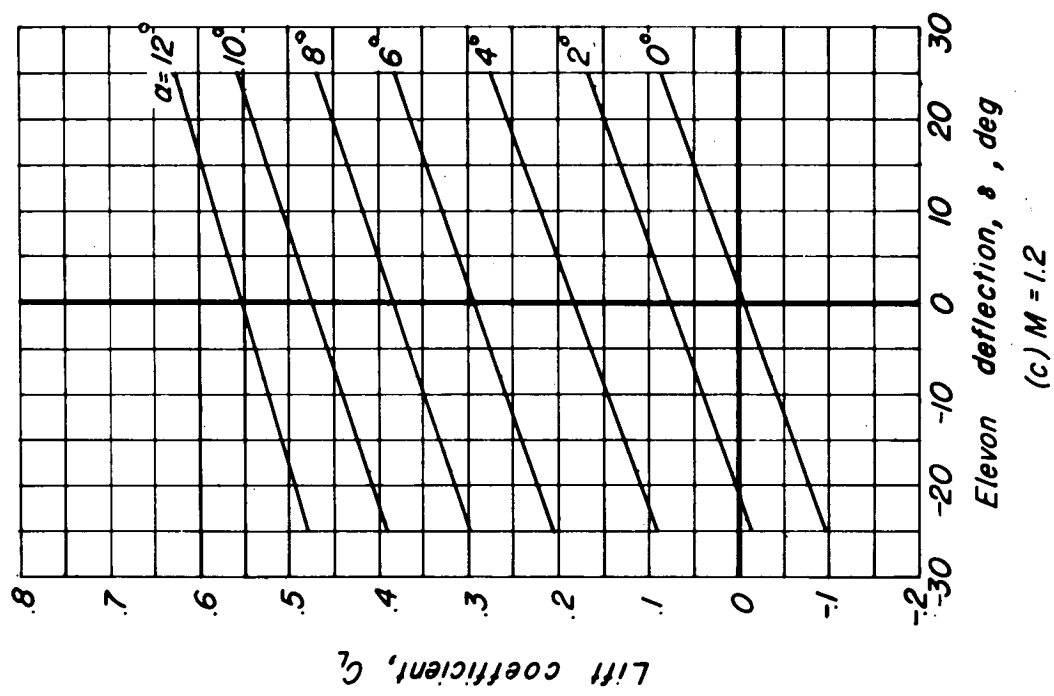


Figure 5.- Concluded.



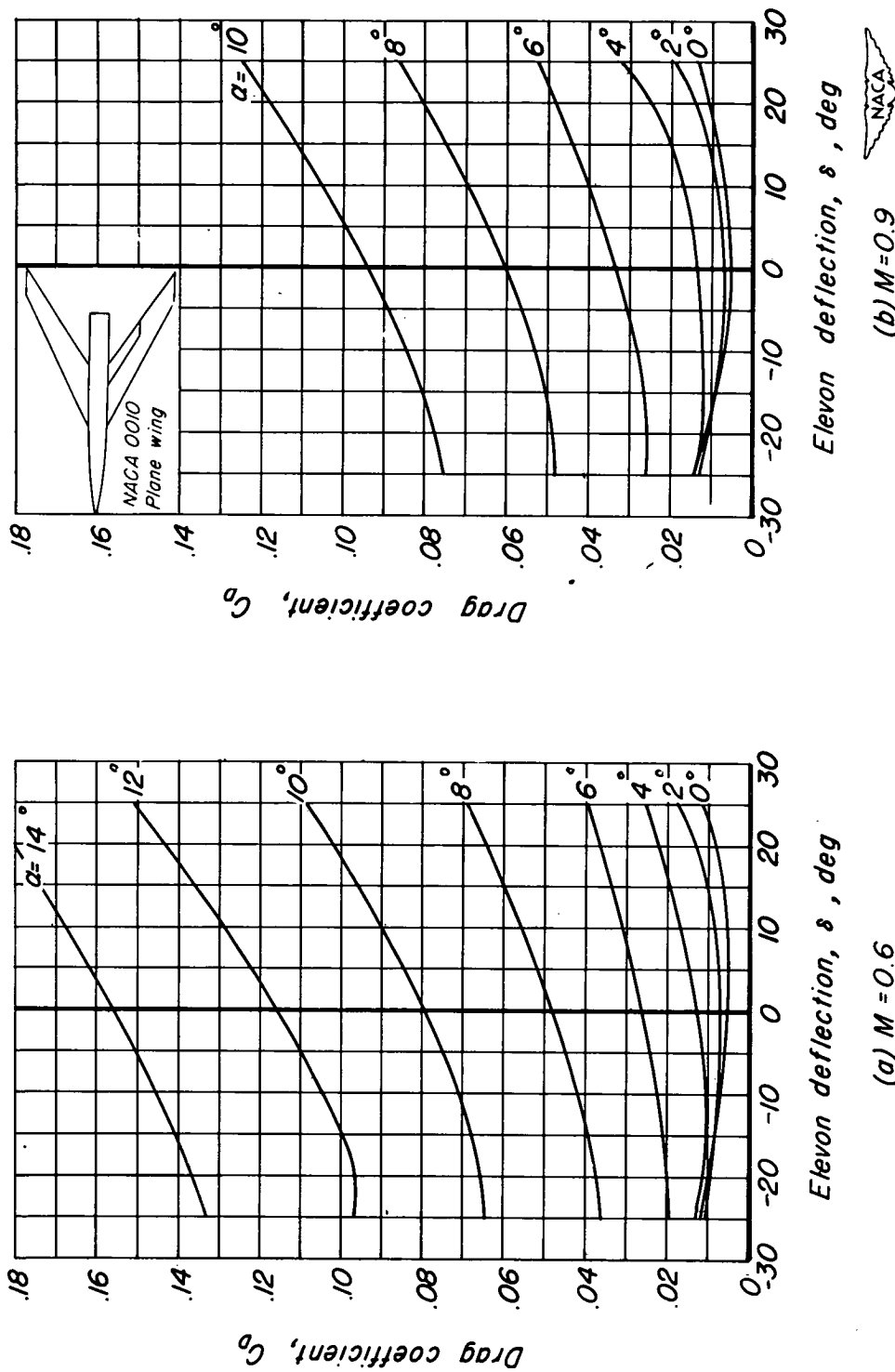


Figure 6.—Variation of drag coefficient with elevon deflection at various Mach numbers.
Data for one elevon. $R = 1.5 \times 10^6$.

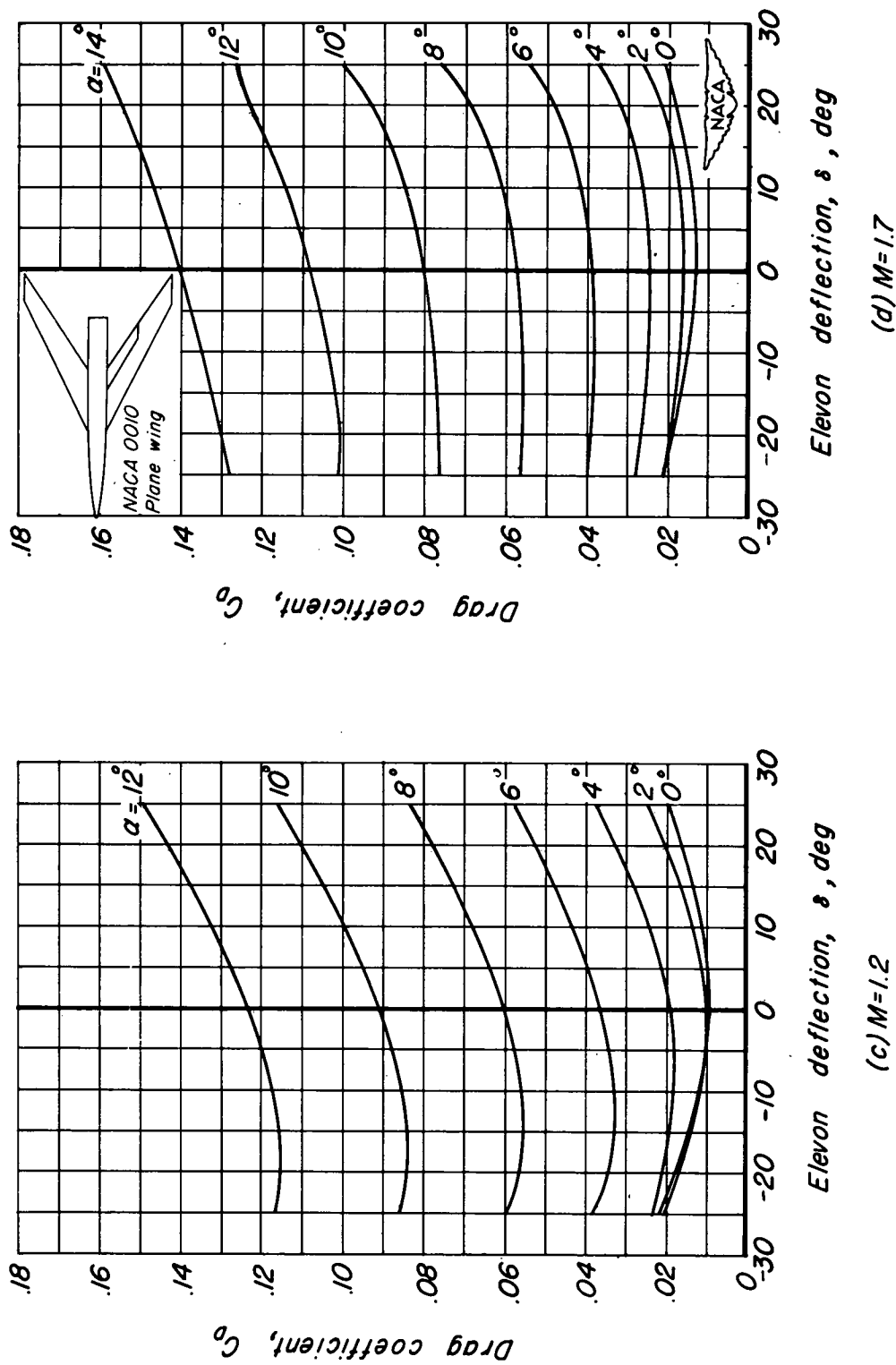


Figure 6.- Concluded.

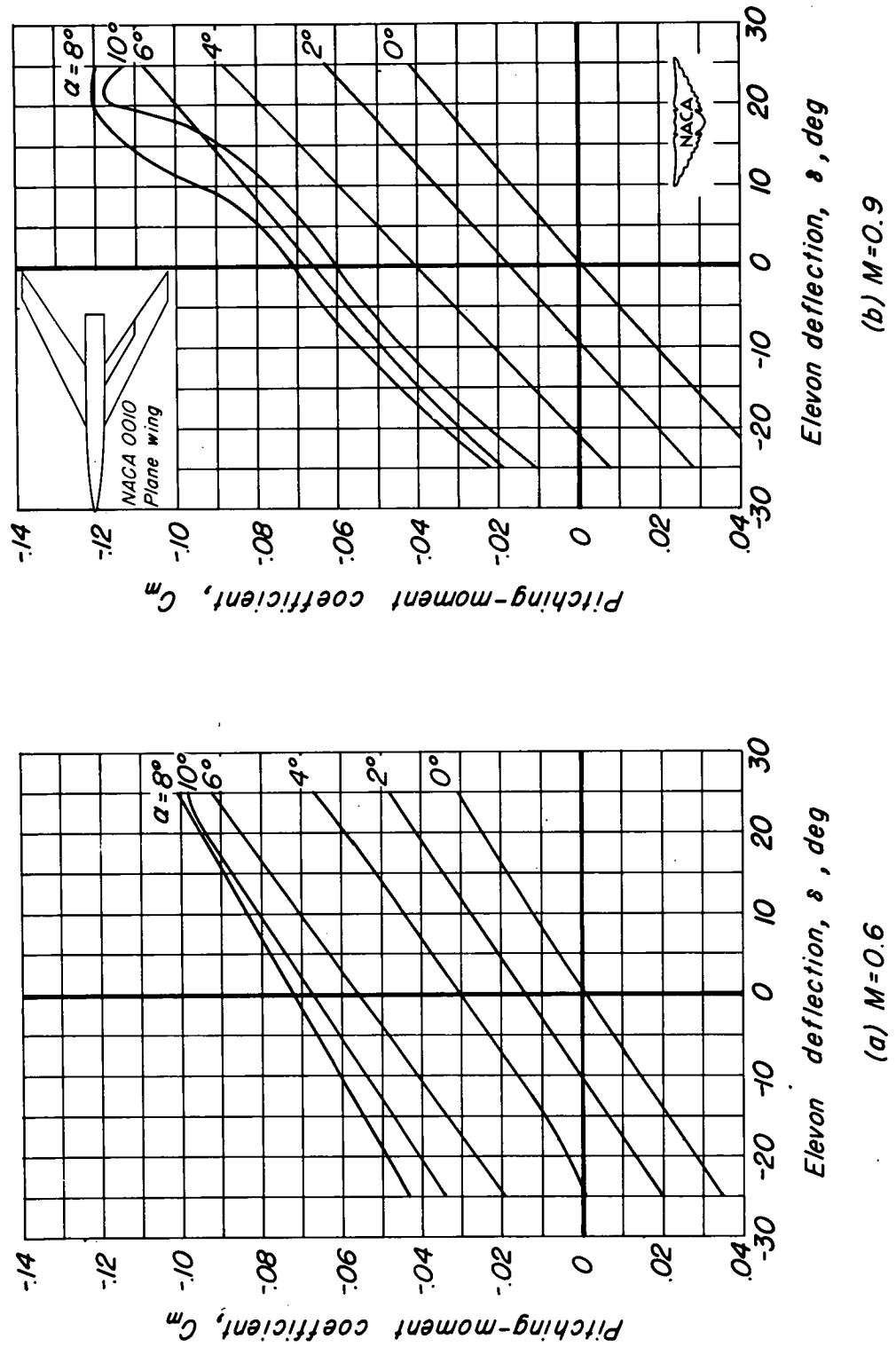


Figure 7. -Variation of pitching-moment coefficient with elevon deflection at various Mach numbers.

Data for one elevon. $R = 1.5 \times 10^6$.

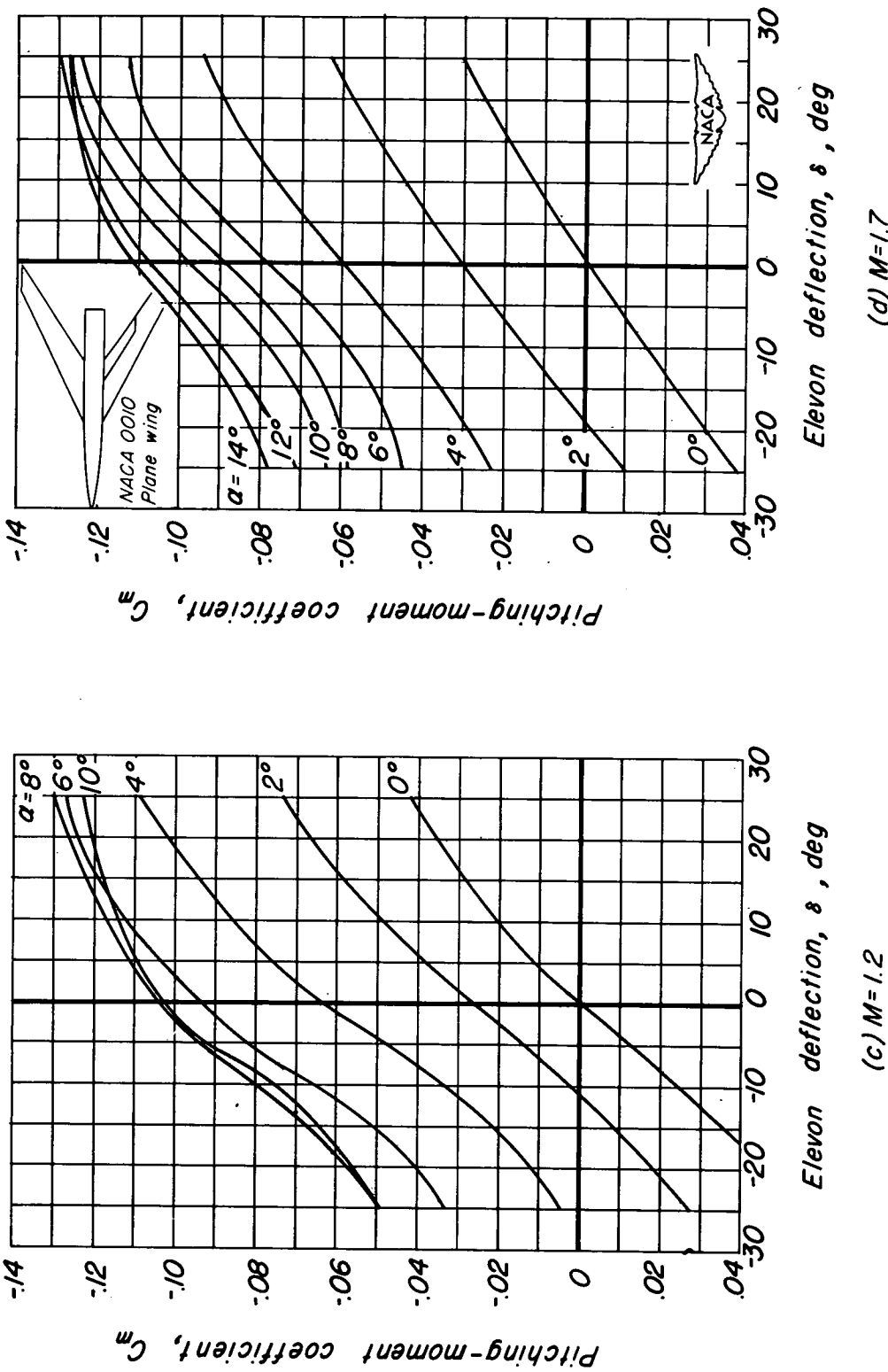


Figure 7. - Concluded.

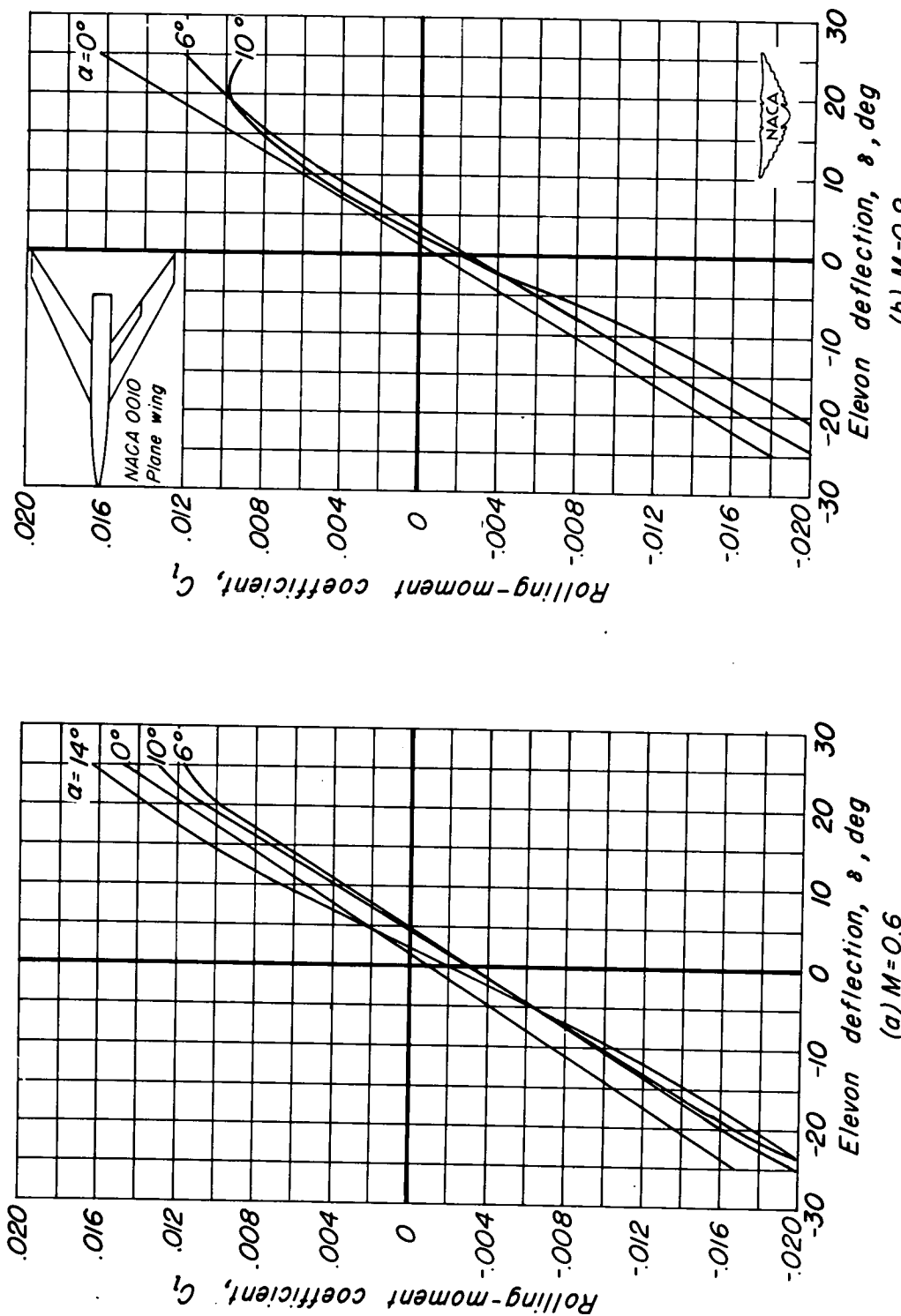


Figure 8. - Variation of rolling-moment coefficient with elevon deflection at various Mach numbers.
Data for one elevon. $R = 1.5 \times 10^6$.

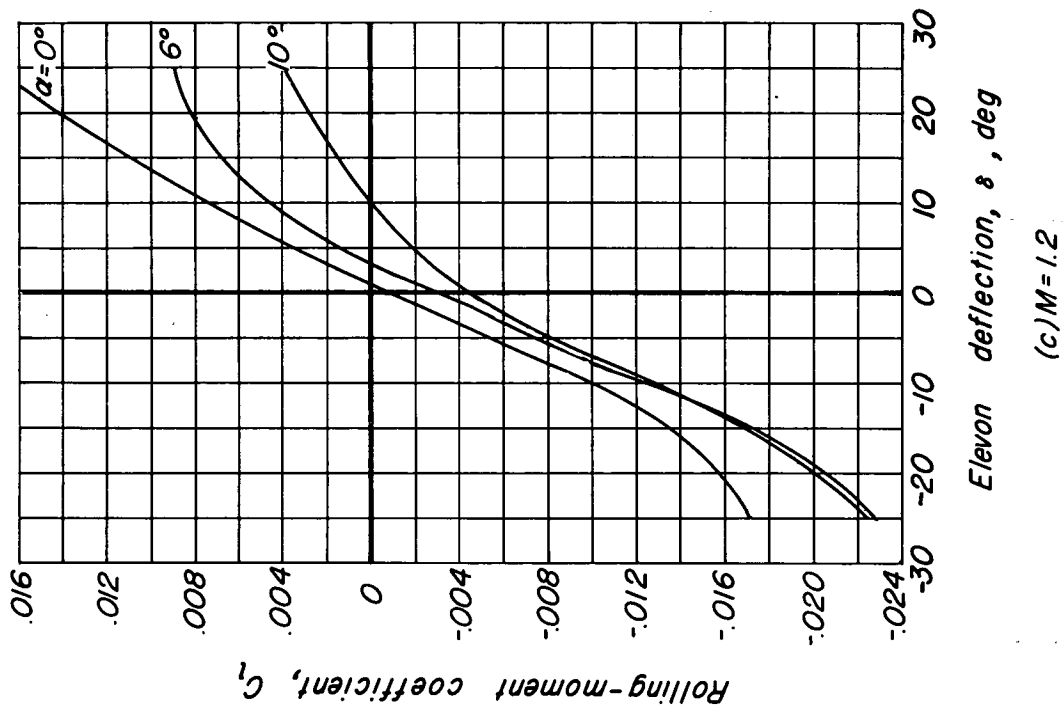
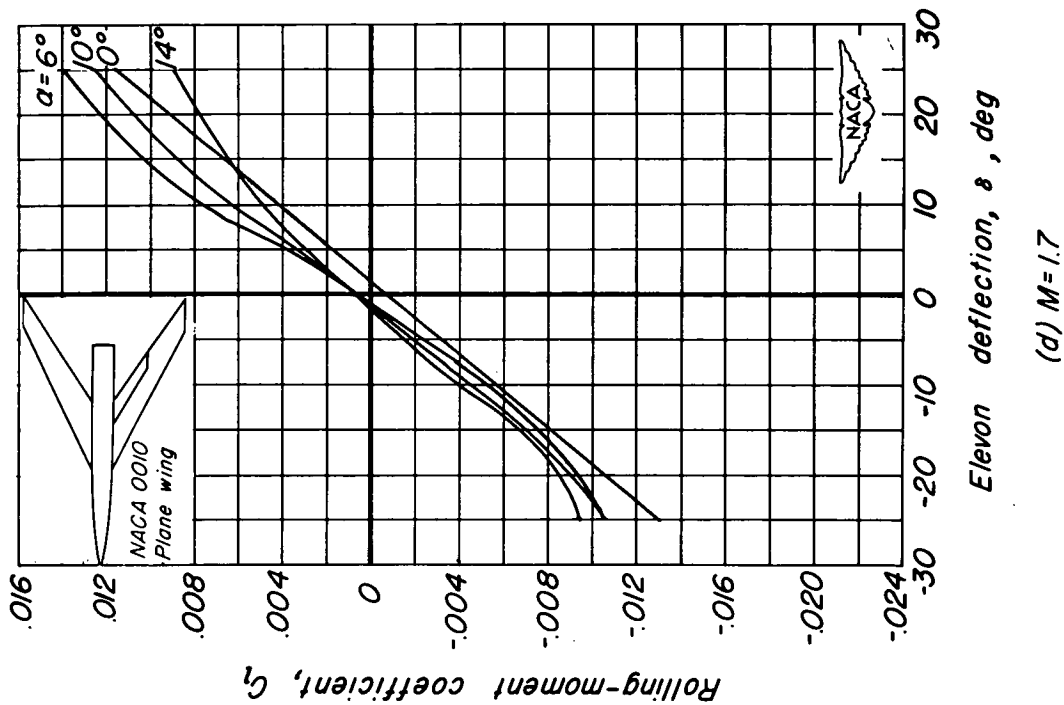
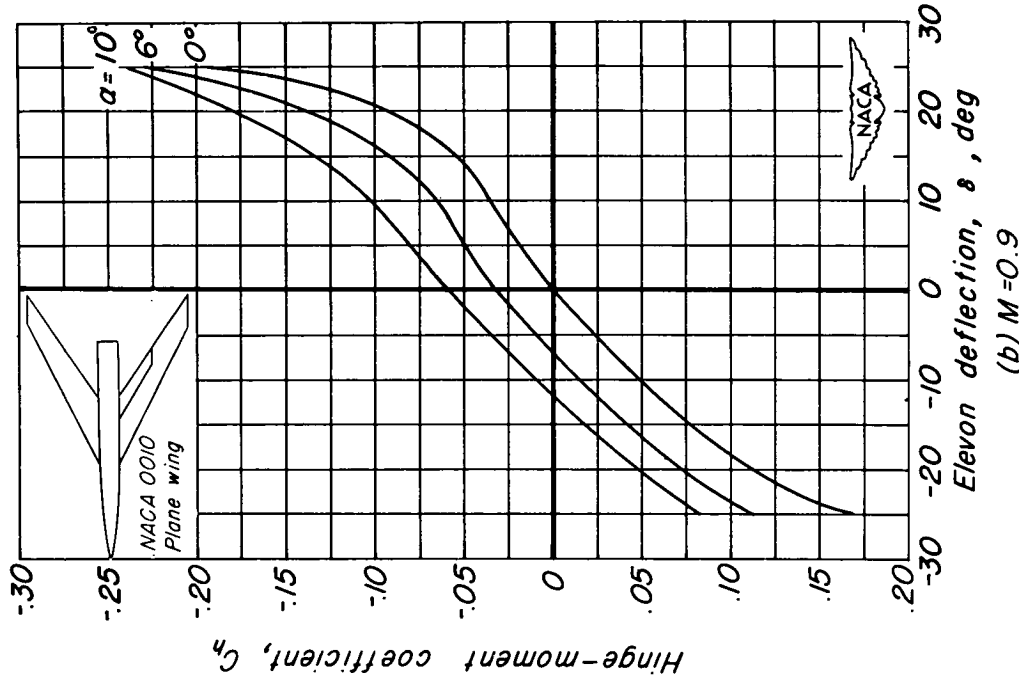
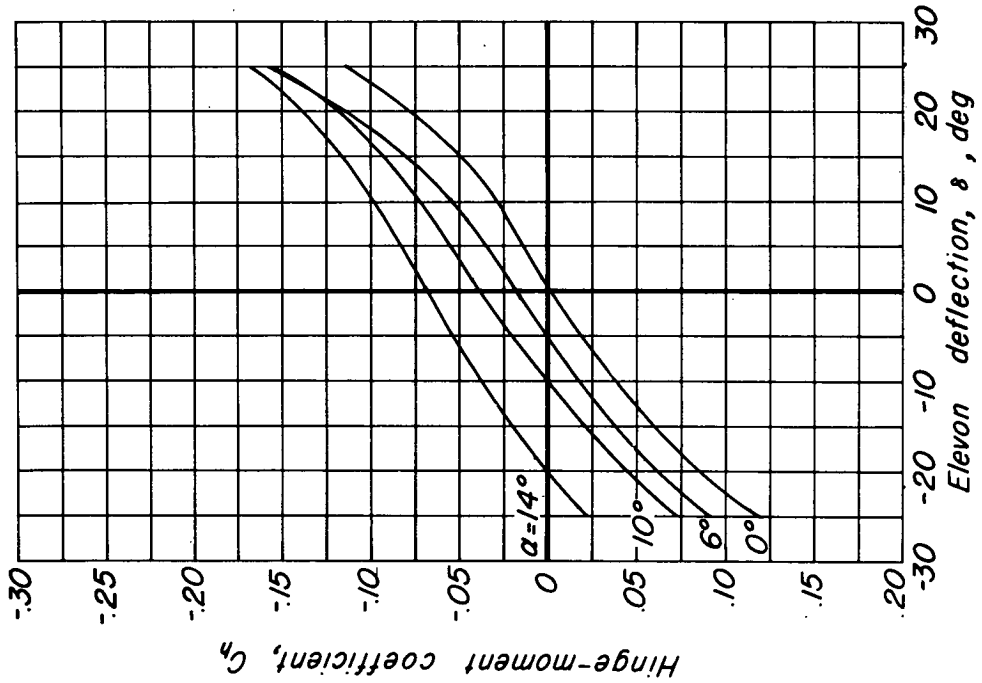


Figure 8. - Concluded.

(a) $M = 0.6$ 

*Figure 9. Variation of hinge-moment coefficient with elevon deflection at various Mach numbers.
Data for one elevon. $R = 1.5 \times 10^6$.*

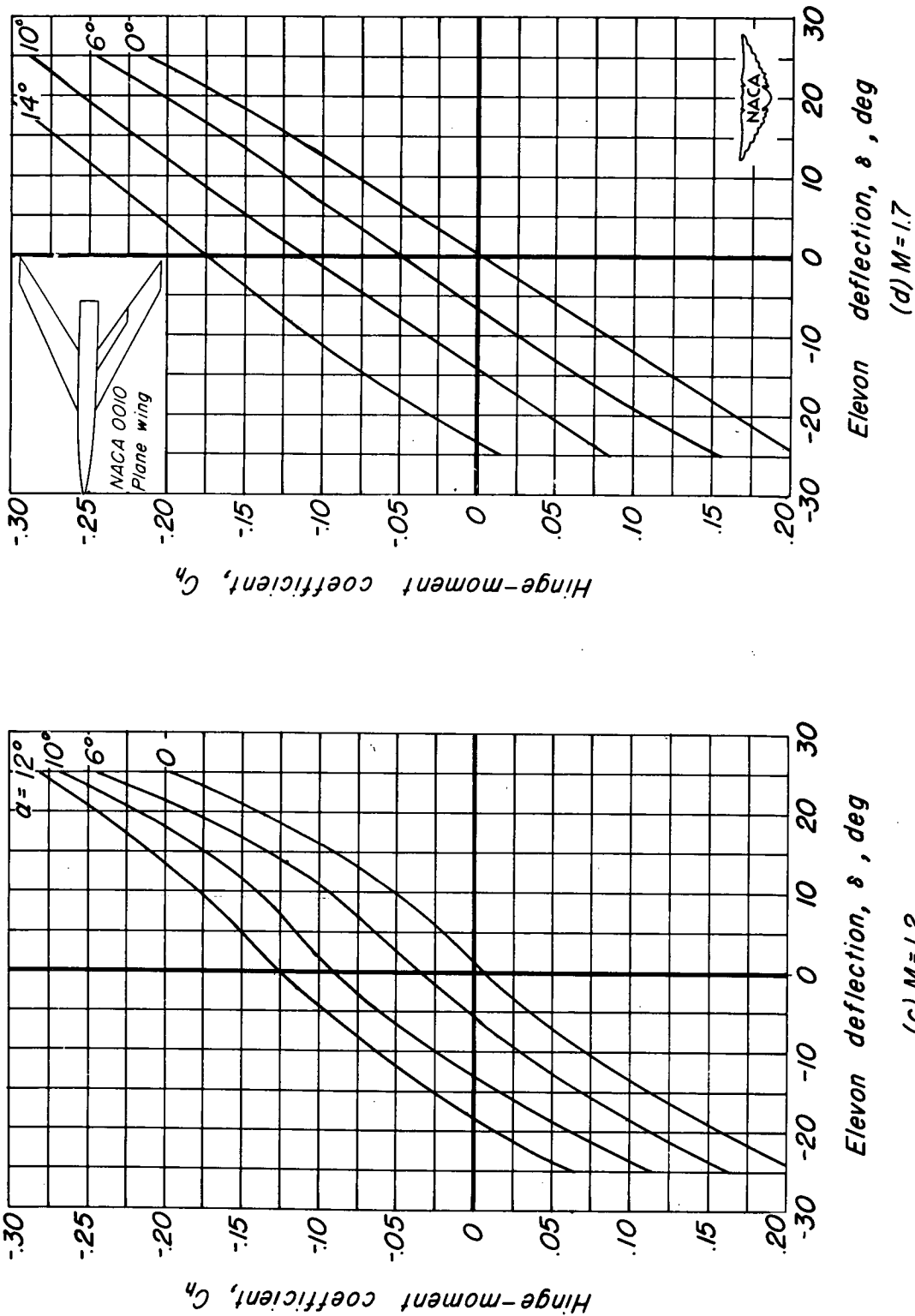


Figure 9. - Concluded.

(c) $M = 1.2$

(d) $M = 1.7$

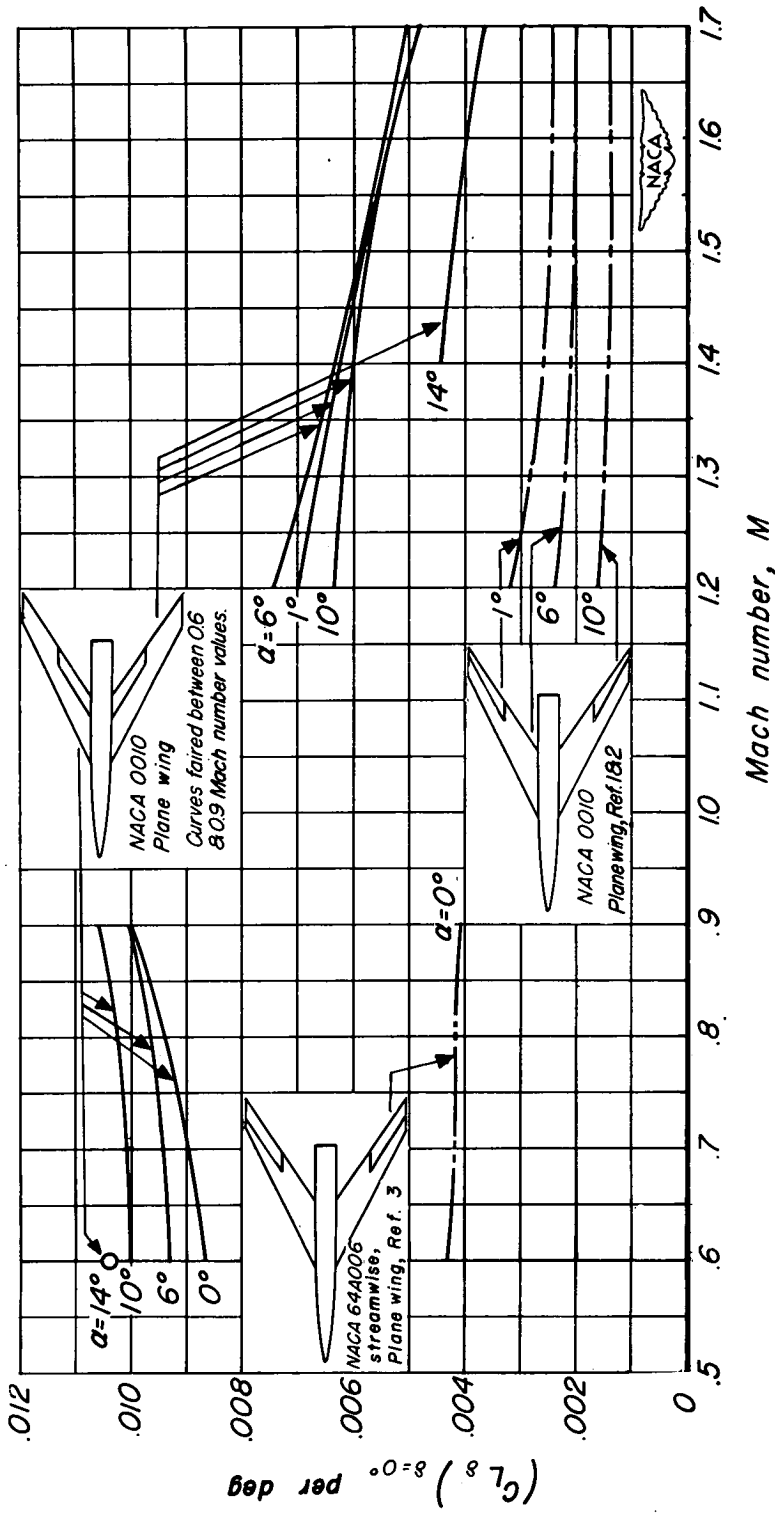


Figure 10.- Variation with Mach number of the lift-effectiveness parameter, C_{Lg} .

Data for two elevons. $R = 1.5 \times 10^6$

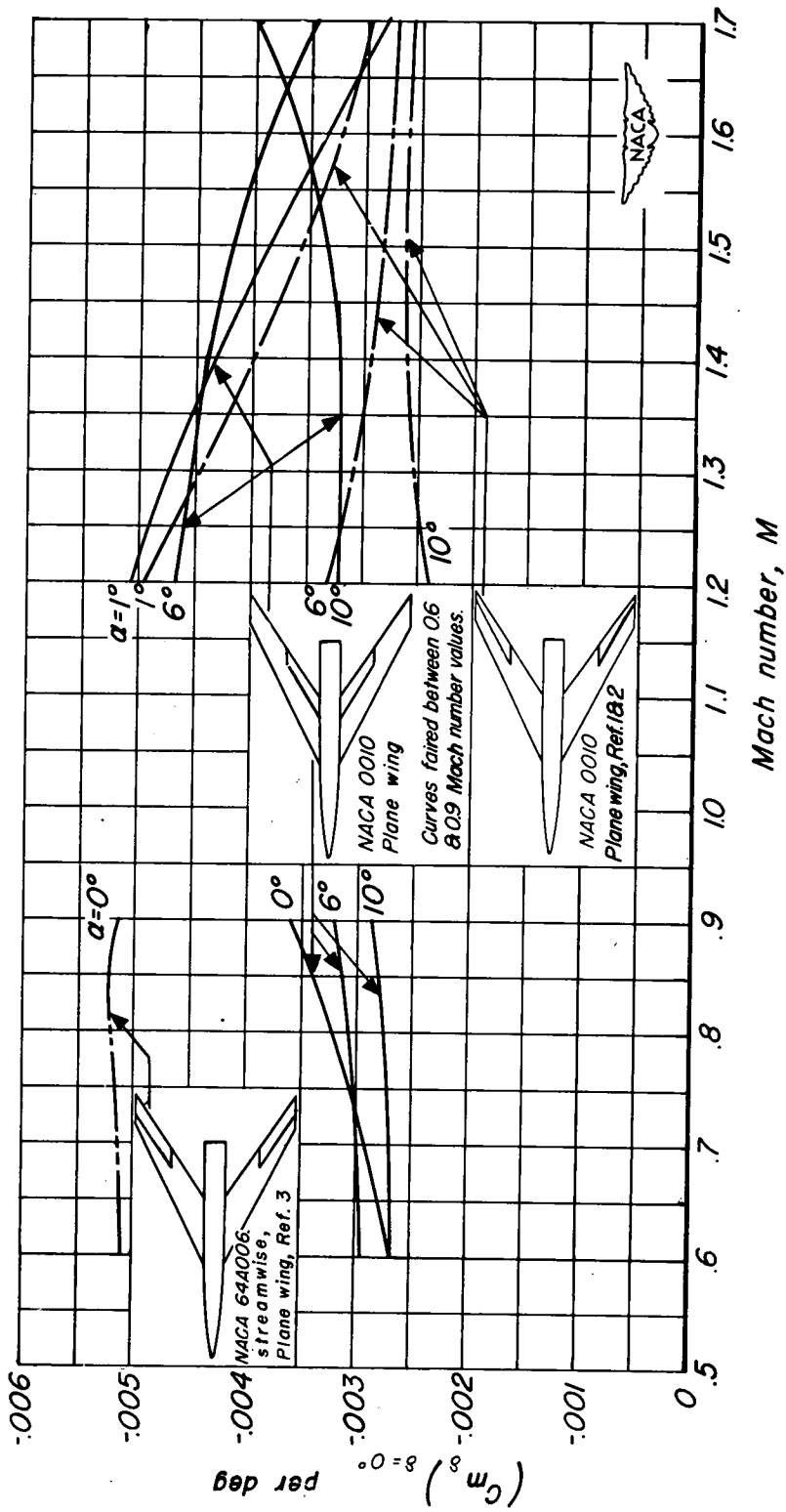


Figure II - Variation with Mach number of the pitching-moment-effectiveness parameter, $C_m g$.

Data for two elevons. $R = 1.5 \times 10^6$.

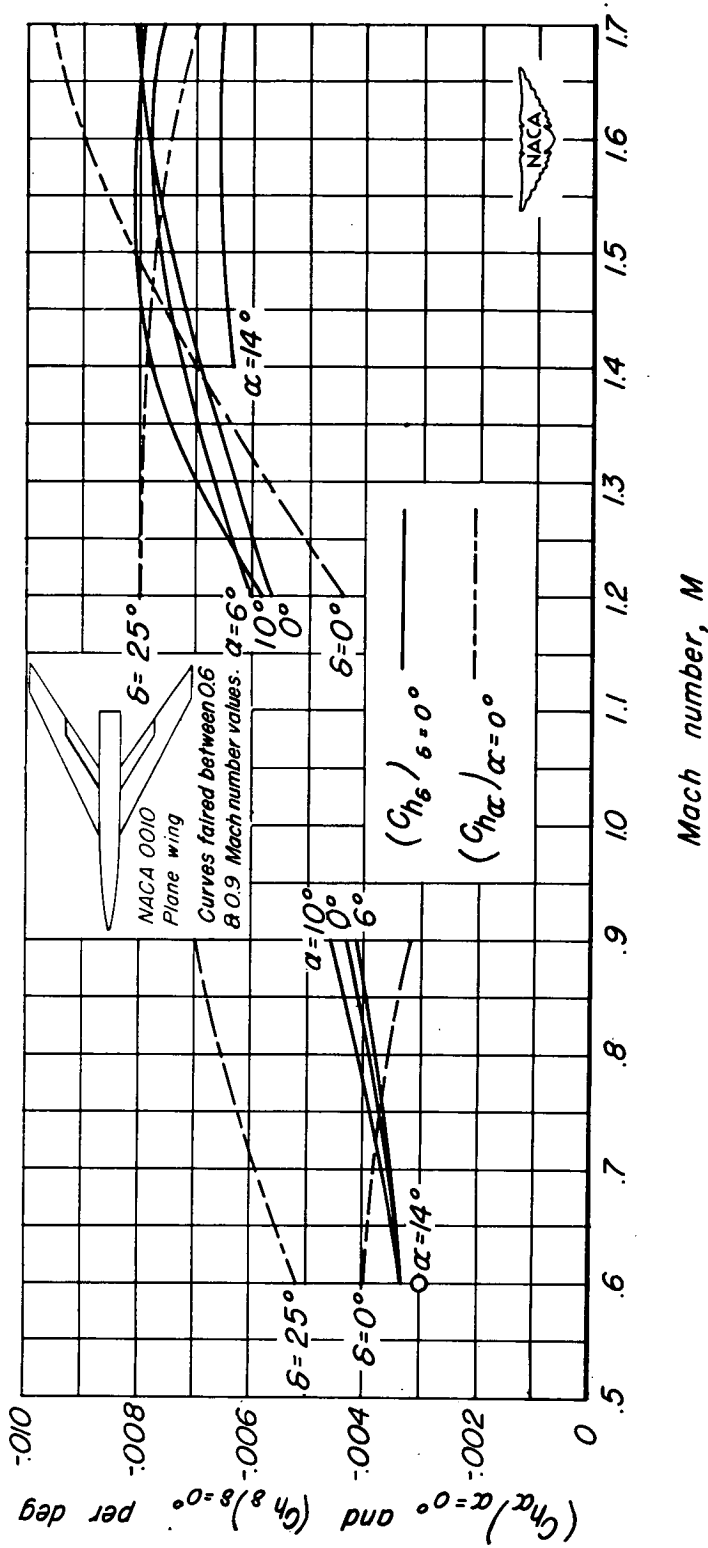


Figure 12.-Variation with Mach number of the rate of change of hinge moment coefficient with change in elevon deflection and angle of attack. $R = 1.5 \times 10^6$.

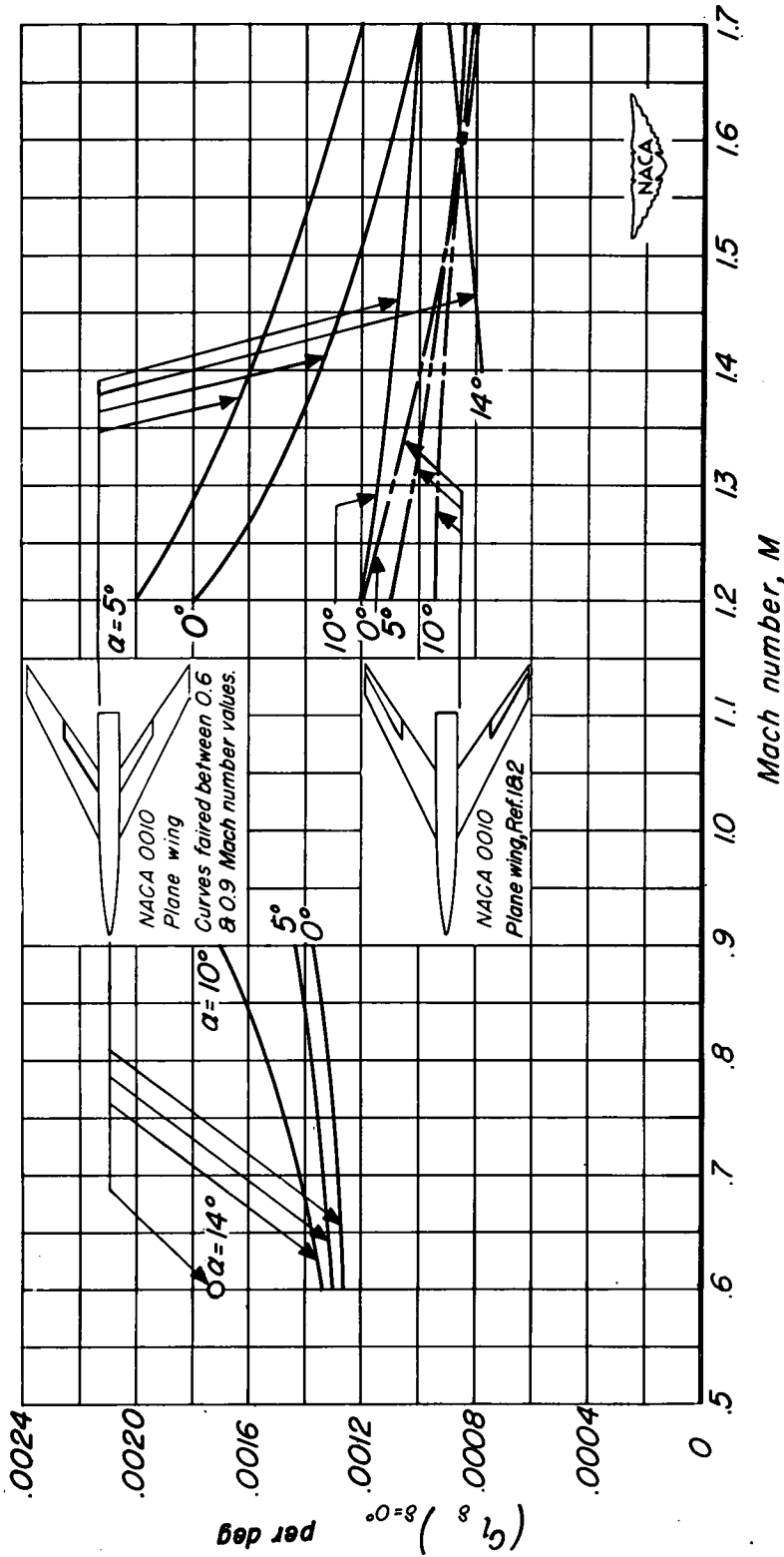


Figure 13.-Variation with Mach number of the rolling-moment-effectiveness parameter C_{l_δ} .

Data for two elevons. $R = 1.5 \times 10^6$.

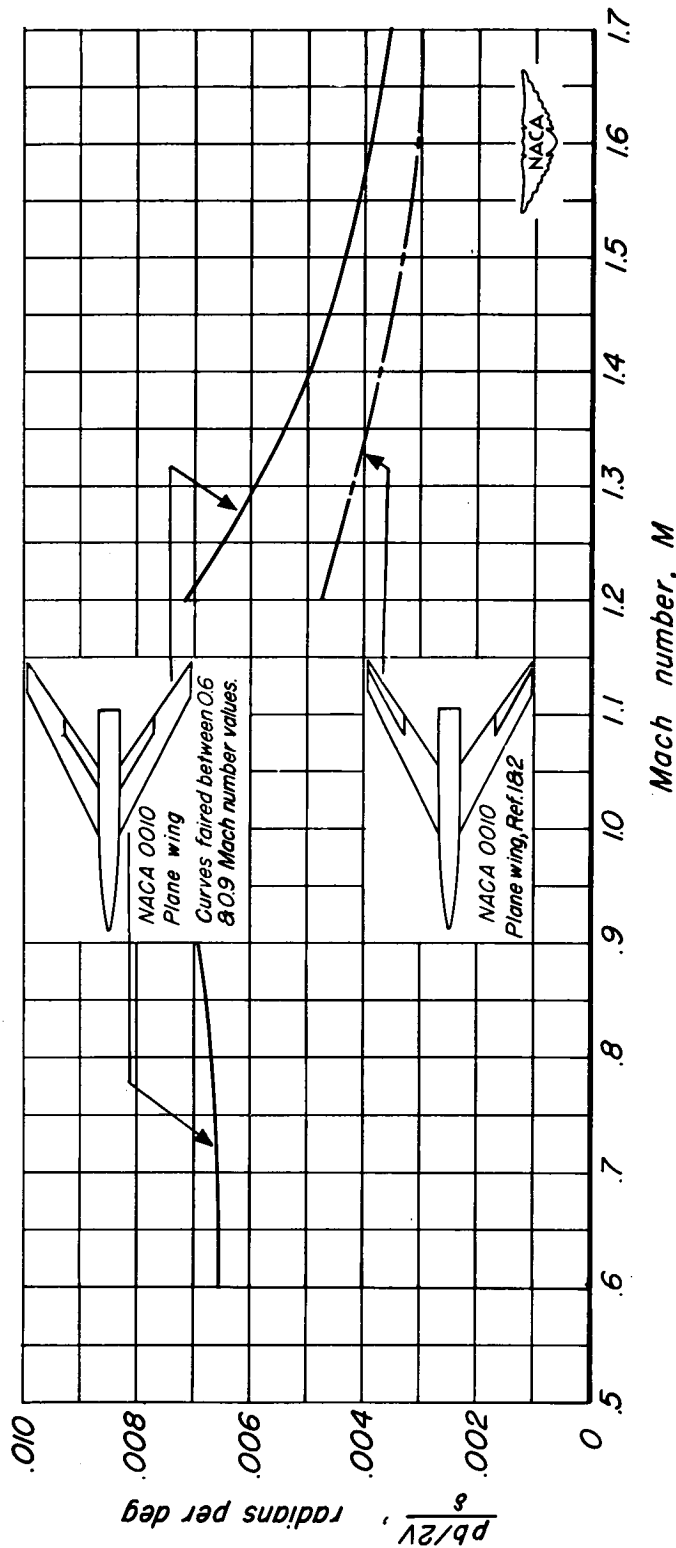


Figure 14. - Variation of the wing-tip helix angle per degree elevon deflection with Mach number. Data for two elevons. $\alpha = 0^\circ$.

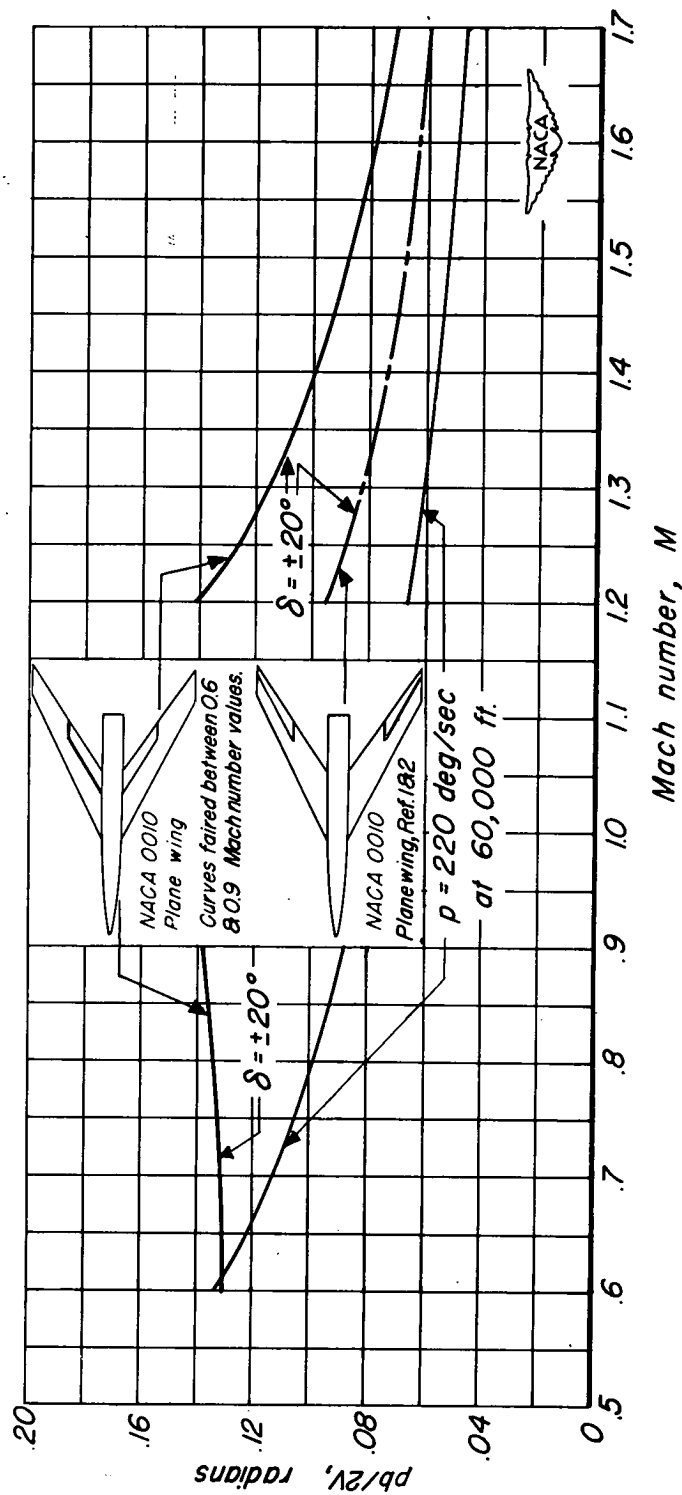


Figure 15.-Comparison of the wing-tip helix angle attainable with 40° total deflection of the elevon with that necessary to produce a wing-tip velocity of 220° per second for a 40-foot-wing-span airplane flying at 60,000 feet. $\alpha = 0^\circ$.